








STOP1-regulated *SMALL AUXIN UP RNA55* (*SAUR55*) is involved in proton/malate co-secretion for Al tolerance in *Arabidopsis*

Raj Kishan Agrahari¹ | Yuriko Kobayashi¹ | Takuo Enomoto¹  |
 Tasuku Miyachi¹  | Marie Sakuma²  | Miki Fujita²  | Takuya Ogata³  |
 Yasunari Fujita^{3,4} | Satoshi Iuchi⁵ | Masatomo Kobayashi⁵  |
 Yoshiharu Y. Yamamoto¹ | Hiroyuki Koyama¹ 

¹Faculty of Applied Biological Sciences, Gifu University, Gifu, Japan

²Mass Spectrometry and Microscopy Unit, RIKEN Center for Sustainable Resource Science, Tsukuba, Ibaraki, Japan

³Biological Resources and Post-harvest Division, Japan International Research Center for Agricultural Sciences (JIRCAS), Tsukuba, Ibaraki, Japan

⁴Graduate School of Life and Environmental Sciences, University of Tsukuba, Tsukuba, Ibaraki, Japan

⁵Experimental Plant Division, RIKEN BioResource Research Center, Tsukuba, Ibaraki, Japan

Correspondence

Hiroyuki Koyama, Applied Biological Sciences, Gifu University, Gifu 501-1193, Japan.
 Email: koyama.hiroyuki.i9@f.gifu-u.ac.jp

Funding information

JSPS KAKENHI, Grant/Award Numbers: 21H02088, 19K05753

Abstract

Proton (H⁺) release is linked to aluminum (Al)-enhanced organic acids (OAs) excretion from the roots under Al rhizotoxicity in plants. It is well-reported that the Al-enhanced organic acid excretion mechanism is regulated by SENSITIVE TO PROTON RHIZOTOXICITY1 (*STOP1*), a zinc-finger TF that regulates major Al tolerance genes. However, the mechanism of H⁺ release linked to OAs excretion under Al stress has not been fully elucidated. Recent physiological and molecular-genetic studies have implicated the involvement of *SMALL AUXIN UP* RNAs (*SAURs*) in the activation of plasma membrane H⁺-ATPases for stress responses in plants. We hypothesized that *STOP1* is involved in the regulation of Al-responsive *SAURs*, which may contribute to the co-secretion of protons and malate under Al stress conditions. In our transcriptome analysis of the roots of the *stop1* (sensitive to proton rhizotoxicity1) mutant, we found that *STOP1* regulates the transcription of one of the *SAURs*, namely *SAUR55*. Furthermore, we observed that the expression of *SAUR55* was induced by Al and repressed in the *STOP1* T-DNA insertion knockout (KO) mutant (*STOP1*-KO). Through in silico analysis, we identified a functional *STOP1*-binding site in the promoter of *SAUR55*. Subsequent in vitro and in vivo studies confirmed that *STOP1* directly binds to the promoter of *SAUR55*. This suggests that *STOP1* directly regulates the expression of *SAUR55* under Al stress. We next examined proton release in the rhizosphere and malate excretion in the T-DNA insertion KO mutant of *SAUR55* (*saur55*), in conjunction with *STOP1*-KO. Both *saur55* and *STOP1*-KO suppressed rhizosphere acidification and malate release under Al stress. Additionally, the root growth of *saur55* was sensitive to Al-containing media. In contrast, the overexpressed line of *SAUR55* enhanced rhizosphere acidification and malate release, leading to increased Al tolerance. These associations with Al tolerance were also observed in natural variations of *Arabidopsis*. These findings demonstrate that

This is an open access article under the terms of the [Creative Commons Attribution-NonCommercial-NoDerivs](https://creativecommons.org/licenses/by-nc-nd/4.0/) License, which permits use and distribution in any medium, provided the original work is properly cited, the use is non-commercial and no modifications or adaptations are made.

© 2023 The Authors. *Plant Direct* published by American Society of Plant Biologists and the Society for Experimental Biology and John Wiley & Sons Ltd.

transcriptional regulation of *SAUR55* by *STOP1* positively regulates H^+ excretion via PM H^+ -ATPase 2 which enhances Al tolerance by malate secretion from the roots of *Arabidopsis*. The activation of PM H^+ -ATPase 2 by *SAUR55* was suggested to be due to PP2C.D2/D5 inhibition by interaction on the plasma membrane with its phosphatase. Furthermore, RNAi-suppression of *NtSTOP1* in tobacco shows suppression of rhizosphere acidification under Al stress, which was associated with the suppression of *SAUR55* orthologs, which are inducible by Al in tobacco. It suggests that transcriptional regulation of Al-inducible *SAURs* by *STOP1* plays a critical role in OAs excretion in several plant species as an Al tolerance mechanism.

KEYWORDS

AHA2, aluminum tolerance, malate secretion, rhizosphere acidification, *SAUR55*, *STOP1*

1 | INTRODUCTION

Aluminum (Al) rhizotoxicity is one of the most serious environmental constraints in acid soils (pH < 5.5), covering over 50% of the world's potentially arable lands (Kochian et al., 2015; Liu et al., 2014). Al tolerance mechanisms have been identified at the molecular level in various plants, which include regulated genes by the *STOP1* transcription factor (see reviews; Daspute et al., 2017; Sadhukhan, Kobayashi et al., 2021). In *Arabidopsis*, the gene for Al tolerance malate transporting *ALMT1* (*Aluminum activated Malate Transporter 1*; Hoekenga et al., 2006) and the citrate transporting *MATE* (*Multidrug And Toxic compound Extrusion 1*; Liu et al., 2009) were identified that they were transcriptionally regulated by *STOP1* (Iuchi et al., 2007; Sawaki et al., 2009). *ALMT1*- and *MATE*-type malate and citrate transporters have been well characterized for their roles in Al tolerance and their regulated nature by *STOP1*-type TFs (transcription factors) (see reviews; Daspute et al., 2017; Wu et al., 2018). In *Arabidopsis*, *STOP1* directly binds to the promoter of *AtALMT1* (Tokizawa et al., 2021) with other TFs corresponding to seven functional *cis*-regions in the promoter, such as the CGCG-box [(Yang & Poovaiah, 2002), a calmodulin-binding/CGCG box DNA-binding protein family involved in multiple signaling pathways in plants] for *CAMTA2* (Calmodulin-binding Transcription Activator 2) (Tokizawa et al., 2015). Such a complex promoter structure would allow the dynamic regulation of transcript levels and pleiotropic roles of OA (organic acid) excretion in stress responses, including Al tolerance and enhanced P-acquisition by chelation of Al and OAs (Wu et al., 2018). In addition, intensive molecular biological studies have uncovered molecular mechanisms underlying Al-inducible activation of *STOP1* (Tokizawa et al., 2015), including posttranslational regulation by ubiquitin ligases (Mercier et al., 2021; Xu et al., 2021; Zhang et al., 2019). However, it is important to understand the molecular mechanism related to coordinate regulation of OA excretion that can additively/synergistically improve Al tolerance.

Physiological studies identified that OA transport is usually coupled with cation transport (e.g., K^+ , H^+), including malate and potassium transport in the guard cells, and malate/citrate and H^+

transport in the root cells (Siao et al., 2020; Zhang et al., 2017). Coordinate transportation of cations and OAs may help to maintain intracellular ion balance (Siao et al., 2020; Yan et al., 2002) as well as to maintain the electrochemical potential of the membrane (Falhof et al., 2016). For example, Shen et al. (2005) demonstrated that Al-induced citrate secretion was mediated via modulation of the activity of the plasma membrane (PM) H^+ -ATPase in a soybean cultivar. A similar model (i.e., coupling with OA transport and H^+ transport) was reported in Al-inducible malate excretion in *Arabidopsis* (Siao et al., 2020; Yu et al., 2016; Zhang et al., 2017) and enhanced citrate excretion in carrot mutant cells that excrete citrate to the medium containing Al-phosphate (Ohno et al., 2003, 2004). Ohno et al. (2003) demonstrated that suppression of H^+ -ATPase by RNAi of a major gene encoding PM H^+ -ATPases at the plasma membrane reduced citrate excretion from the carrot mutant cell line that can utilize Al-phosphate as a P-source by enhanced citrate excretion. In addition, a reverse genetic study in *Arabidopsis* identified that a gene encoding major PM H^+ -ATPase in *Arabidopsis*, namely *AHA2*, plays a crucial role in H^+ -release and elongation of the roots under phosphate deficiency and Al rhizotoxicity (Yuan et al., 2017; Zhang et al., 2019). These studies revealed an association between OA and H^+ release, while it remained unclear whether these events are coordinately regulated by the same pathway, such as the *STOP1*-dependent pathway of transcriptional regulation.

Previous studies of *STOP1*-like proteins revealed co-regulation of the expression of sets of genes, which systemically control Al tolerance by coordinately regulating functionally related molecules. For example, the rice ortholog of *STOP1*, namely *ART1* (*Aluminum Resistance Transcription factor 1*), regulates the expression of *STAR1* (for *Sensitive To Al Rhizotoxicity 1*)/*STAR2*, which are co-expressed together and encode a subunit of the half-type ABC transporter for Al tolerance (Huang et al., 2009). By contrast, the ATTED-II database (<http://atted.jp/>; Obayashi et al., 2022) identified the co-expression gene network with *AtALMT1* in *Arabidopsis* some of which are directly regulated by *STOP1* (Figure 1). The co-expression genes network of *AtALMT1* contains a unique homolog of *STOP1* in *Arabidopsis*, namely *STOP2* that regulates the transcription of several genes for H^+ -tolerance (Kobayashi

et al., 2014), a gene for potassium transporter *HAK5* (High-Affinity K^+ transporter 5), and *PGIP1* (Polygalacturonase-inhibiting protein 1), which contribute Al and H^+ -tolerance (Agrahari et al., 2021; Kobayashi et al., 2014; Sawaki et al., 2009). These genes were reported as the direct targets of STOP1 (i.e., carrying functional STOP1-binding cis-element; Tokizawa et al., 2021). Other members belonging to the co-expression network might contribute to Al and H^+ -tolerance, including the regulation of malate excretion by *ALMT1*. For example, one of the members of *SMALL AUXIN UP-RNA* (*SAUR*), consisting of 79 members in the Arabidopsis genome (Spartz et al., 2014), was identified in the co-expression genes network of *AtALMT1*. Originally, *SAURs* were identified as positive regulators of the PM H^+ -ATPase including *AHA2* in response to IAA, but the different responses of several *SAURs* have recently been reported under diverse stress conditions (Ren & Gray, 2015). For example, Qiu et al. (2020) reported ABA-responsive *SAUR41* to modulate cell expansion, ion homeostasis, and salt tolerance in Arabidopsis which are mediated by H^+ release regulated by H^+ -ATPases. Furthermore, Wang et al. (2021) reported the involvement of *SAUR26* in varying the thermo-responsiveness of Arabidopsis accessions' growth architecture. These studies suggest that co-expressing *SAUR* (e.g., *SAUR55*) with *AtALMT1* may have a role in Al tolerance by regulating the co-transport of H^+ and malate in Arabidopsis.

In the current study, we identified that the STOP1 coordinately regulates the Al-inducible expression of *AtALMT1* and *SAUR55*, which modulates *ALMT1*-dependent malate excretion under Al-toxic conditions. Among the *SAUR* family, *SAUR55* was uniquely upregulated by Al, and that was regulated by STOP1 in Arabidopsis. This suggests that STOP1-regulated *SAUR55* is involved in the Al-induced malate excretion mechanism for Al tolerance in Arabidopsis, which is mediated by a plasma membrane co-transport system in which H^+ -ATPase and *ALMT1* are coupled.

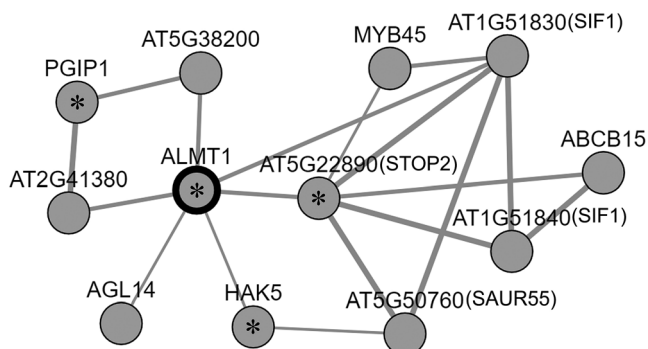


FIGURE 1 Co-expression network of *AtALMT1*. The co-expression network was constructed by the network drawer tool (with the Coex option to add many genes i.e., automatically adding genes around query genes) of the ATTED-II database using *AtALMT1* as a query gene. Genes that have been previously reported as being regulated by STOP1 such as *AtALMT1* (Tokizawa et al., 2015), *STOP2* (Kobayashi et al., 2014; Tokizawa et al., 2021), *PGIP1* (Agrahari et al., 2021), and *HAK5* (Sawaki et al., 2009) are indicated by asterisks.

2 | RESULTS

2.1 | Profiling of *SAUR55* expression under Al stressed conditions

To investigate whether *SAUR55* is inducible by Al and downstream of STOP1, we profiled the expression of *SAUR55* using our previous transcriptome data (Sawaki et al., 2009) (Figure 2a). Using fold change (FC) values, all *SAUR* family gene expression levels were compared with Al. Most *SAURs* were not inducible by Al; however, *SAUR55* showed Al inducible expression with the highest FC (around four times) along with the other Al inducible *SAUR33*. Among Al-inducible *SAURs*, *SAUR55* showed lower expression levels in the *stop1* mutant (essential domain of STOP1 i.e., Cys₂His₂ includes a missense mutation; Iuchi et al., 2007), while *SAUR33* expression was unchanged in the *stop1* mutant. Contrastingly, the expression of *SAURs* has been reported responding to IAA or ABA (Ren & Gray, 2015; Spartz et al., 2012, 2014). Therefore, we analyzed the IAA and ABA-responsive expression of the *SAUR* family genes using public transcriptome data. Expression of several groups of *SAURs* (based on AA similarity), including *SAUR33*, were responsive to IAA or ABA, whereas *SAUR55* remained nonresponsive to either (Figure S1A). Furthermore, RT-qPCR data confirmed that the expression of *SAUR55* did not respond to IAA or ABA (Figure S1B) when compared to *SAUR19* (Spartz et al., 2012) and *SAUR41* (Qiu et al., 2020), which are highly responsive to both IAA and ABA. These results indicated that *SAUR55* is Al inducible but not responsive to IAA or ABA and is regulated by STOP1.

Al dose-dependent and time course analyses also showed that the expression of *SAUR55* was induced by Al (Figure 2b,c). When the expression levels of *SAUR55* were compared at 24 h of Al treatment, the expression of *SAUR55* in the T-DNA insertion knockout (KO) mutants of STOP1 (*STOP1-KO*) was about 20% of that of the wild-type ecotype Columbia (Col-0). By contrast, a similar expression level was found in the *stop1* mutant and *STOP1-KO* (Figure 2d). Furthermore, the expression of *SAUR55* was recovered in the *STOP1*-complemented transgenic plant (Figure 2d). In addition, the expression of *SAURs* (*SAUR74*, *76*, *77*, *78*, and *79*) belonging to the nearest neighbors of *SAUR55* in the phylogenetic tree (Figure 2a; Ren & Gray, 2015) were not suppressed in the *STOP1-KO* compared with the wild-type (Figure S2). These results indicate that *SAUR55* is downstream of the STOP1 system and unique from the other *SAURs* in the *SAUR* family.

Tissue-specific expression patterns of *SAUR55* were analyzed using stable transformants of *SAUR55* promoter::*GUS* transgenic plants. The *GUS* activity and expression were weaker in roots at the early time point (3 h and 6 h) of Al stress (Figure 2e,f). In contrast, early Al stress treatment *GUS* activity was first observed at the elongation zone (3 h) and root tips (6 h) (Figure 2e). However, after 24 h Al stress, the intensity of *GUS* activity was substantially increased throughout the seedlings (Figure 2e).

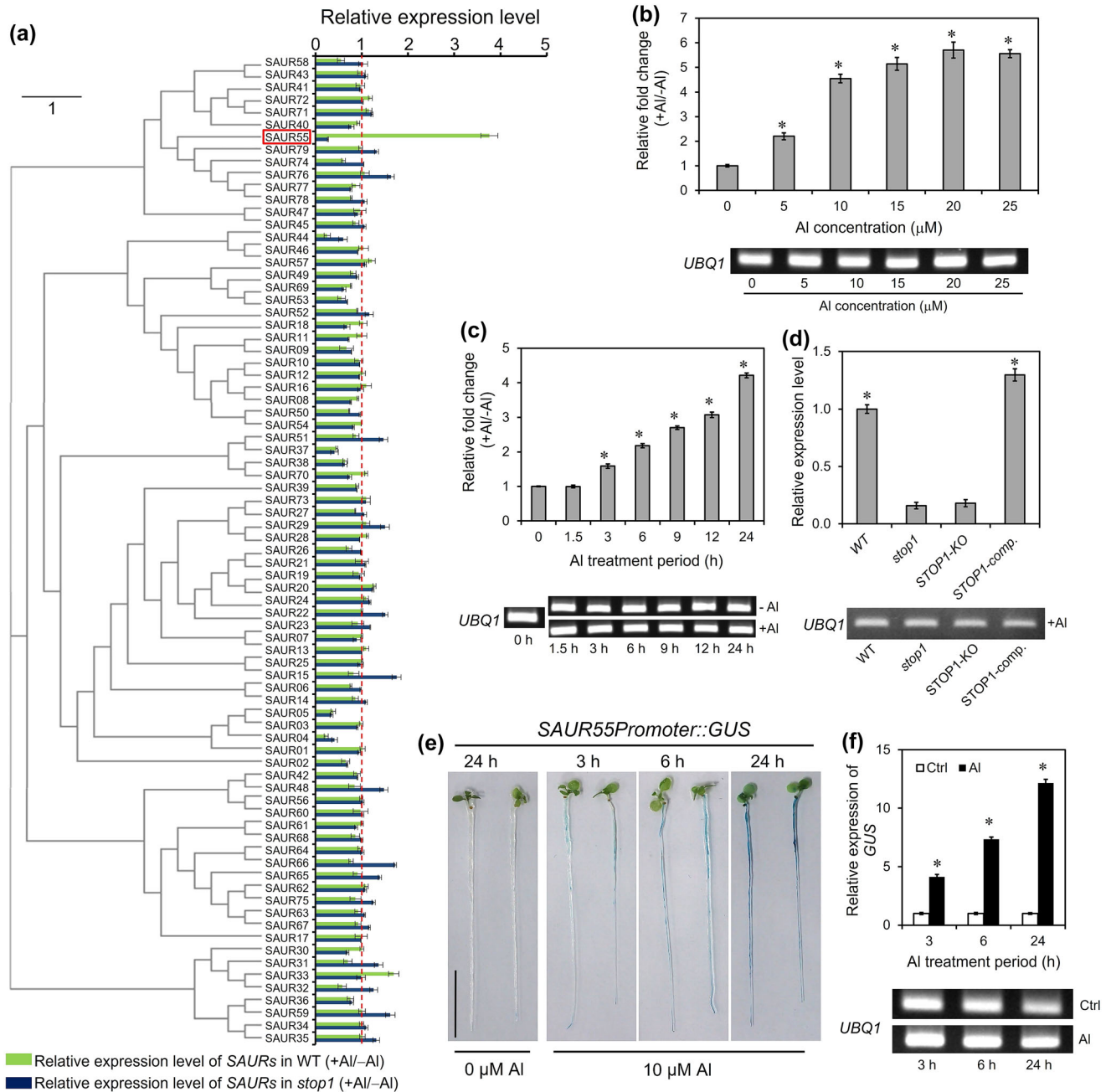


FIGURE 2 Transcriptomic analysis for Al-inducible *STOP1* regulated *SAUR55*. (a) Relative expression levels of the *SAURs* family in wild-type (WT, Col-0) and *STOP1* mutant (*stop1*) under control (-Al) and Al stress treatment for 24 h are shown. The phylogenetic tree of the *SAURs* was constructed by MEGA 6.0 using the neighbor-joining method. The expression data in the root was obtained from our previous microarray data (Sawaki et al., 2009). The dotted line represents the ratio of gene expression with Al to that without Al. The red color box indicated the unique expression nature of *SAUR55* which shows significant induction under Al stress (Student's *t*-test, $P < .05$). (b) Dose-response of *SAUR55* in roots treated with different concentrations of Al for 24 h. (c) Time-dependent expression of *SAUR55* in root in response to Al (10 μ M AlCl₃ at pH 5.0) for different time periods. The roots were excised from the 10 days of pre-grown WT plants exposed to different treatments. Relative fold change was calculated as the ratio of gene expression with Al to that without Al. (d) Transcriptional regulation of *SAUR55* by *STOP1* is shown. *SAUR55* expression was quantified in 10 days of pre-grown seedlings of WT, *stop1*, *STOP1-KO*, and *STOP1-comp.* treated with Al (10 μ M AlCl₃ at pH 5.0) for 24 h. The data represent relative expression level compared to the WT (e) *SAUR55* promoter::GUS reporter assays in roots. Roots of 10 days old transgenic plants carrying *GUS* gene driven by *SAUR55* promoter were exposed to control (0 μ M AlCl₃ at pH 5.0) and Al-containing (10 μ M AlCl₃ at pH 5.0) solutions for different time periods. Bar = 5 mm. (f) *GUS* expression levels were quantified in Arabidopsis transgenic lines carrying *SAUR55* promoter::GUS in response to Al (10 μ M AlCl₃ at pH 5.0) at different time periods. The expression levels were measured by qRT-PCR. *UBQ1* was used for normalizing the gene expression level. The average values of three biological replicates are presented with standard errors. An asterisk indicates a significant difference (Student's *t*-test, $P < .05$). Semi-quantitative PCR bands of *UBQ1* are shown. PCR products were separated by 3% agarose gel electrophoresis and visualized with GelRed staining.

2.2 | STOP1-mediated SAUR55 expression

Our previous studies have shown that *ALMT1*, *PGIP1*, and *STOP2*, which form a co-expression gene network with *SAUR55*, carry functional STOP1-binding sites in the promoter (Agrahari et al., 2021; Tokizawa et al., 2015, 2021). To identify a similar STOP1-binding site in the promoter of *SAUR55*, we conducted an *in vitro* competitive STOP1-binding assay. The putative STOP1-binding sites in the promoters of *SAUR55* were inferred using the Plant Cistrome Database, which cataloged the DNA sequence of the regulatory region of the promoter, which was analyzed by DNA affinity purification sequencing method with various transcription factors (O'Malley et al., 2016). The *SAUR55* promoter had one STOP1 interacting region (−1,480 to

−1,441 bp from the first ATG) of the cistrome database (Figure 3a), which contained two GGNVS minimum consensus (Tsutsui et al., 2011) of the STOP1/ART1 binding element (Figure 3a). A 40-bp synthetic double-stranded DNA probe designed at the putative STOP1-binding site of the *SAUR55* promoter (−1,480 to −1,441 bp) was found to compete with a known STOP1-binding dsDNA sequence of the *ALMT1* promoter (Tokizawa et al., 2015). However, a mutation in one of the “GGNVS” consensus sequences (designated as *CIS-D mutated-2*) abolished STOP1 binding capacity. By contrast, a mutation in the other GGNVS consensus regions (designated as *CIS-D mutated-1*) competes with the positive dsDNA obtained from *ALMT1* (Figure 3b). In addition, this region was also validated by the *in planta* assays using the transgenic hairy root of *Arabidopsis* transformed with

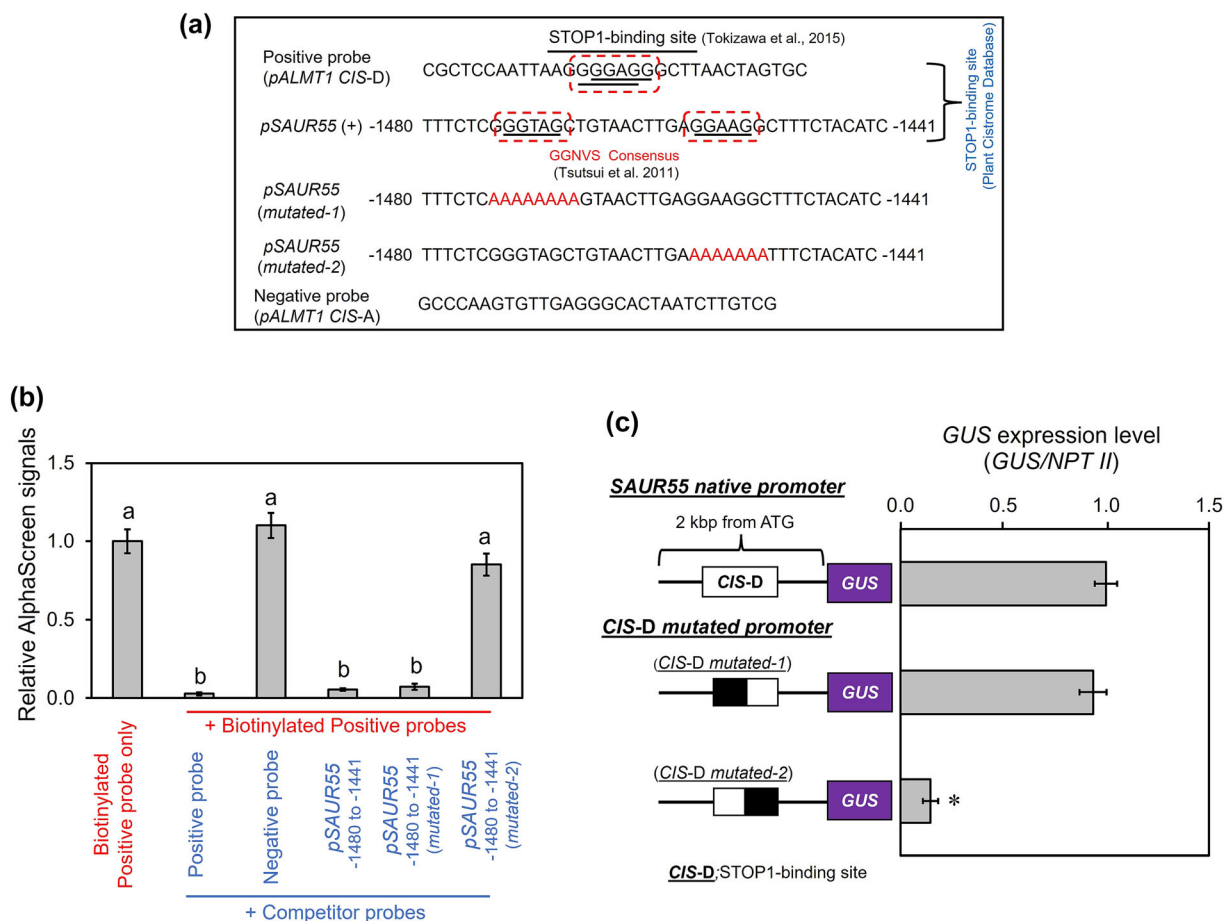


FIGURE 3 *SAUR55* regulation by STOP1. (a) The STOP1-binding sites of *SAUR55* promoter were retrieved from the Plant Cistrome Database. The dotted boxes indicate the GGNVS sequences that represent the STOP1-ortholog ART1 binding minimum consensus. STOP1 binding (*CIS-D*) and non-binding (*CIS-A*) sites on the *ALMT1* promoter were utilized as positive and negative control probes, respectively (Tokizawa et al., 2015). *SAUR55* mutated probes were designed by replacing the GGNVS consensus sequence with stretches of A/T (shown in red font). (b) Bar graph representing the *in vitro* competitive binding assay of translated STOP1 protein with the synthetic double-stranded promoter fragments was performed by using the PerkinElmer Amplified Luminescent Proximity Homogeneous Assay (AlphaScreen™). Competitive binding assay was performed using 450 nM competitor probes (shown in blue font) which compete with 50 nM biotinylated positive probes (shown in red font) for binding with the STOP1. The graph represents the emitted light signal intensities relative to the biotinylated probe without any competitors. Lower emitted signal intensity signifies the binding of the STOP1 protein to the respective competitor probe. Data presented as the means of three biological replicated ($n = 3$) with standard error (SE). Different letters indicate significant differences (Tukey's test, $P < .05$) in emission intensity. (c) *GUS* expression in *Arabidopsis* transgenic hairy roots expressing *SAUR55* promoter::*GUS*, which have native and mutated (*CIS-D mutated-1* and *CIS-D mutated-2*) forms of STOP1-binding region. Twenty to thirty transgenic hairy roots were treated with AI stress solution (10 μM AlCl_3 at pH 5.0) for 24 h. Gene expression is normalized to *NPT II*. Average values \pm SE ($n = 3$) are presented. The asterisk indicates a significant difference as determined by Student's *t*-test ($P < .05$).

the *SAUR55* native promoter::GUS or the mutated promoter::GUS (Figure 3c). The GUS expression of the *SAUR55* native promoter (−2000 bp from the transcription start site) showed a significantly higher level of induction than that of the mutation-induced promoter (*CIS-D mutated-2*) (Figure 3c). These results indicated that the induction level of *SAUR55* under Al was directly regulated by the binding of STOP1 to its promoter.

2.3 | Rhizosphere acidification in *STOP1*-KO and *saur55*

We assessed the involvement of STOP1 and *SAUR55* to regulate the H⁺ release from the roots under Al stress by the rhizosphere acidification assay using bromocresol purple, which is an acidic pH indicator with a yellow color at pH < 5.5 (Spartz et al., 2014). The rhizosphere acidification of Arabidopsis pre-treated with Al (10 μM AlCl₃ at pH 5.0) or without Al (0 μM AlCl₃ at pH 5.0) for 24 h was visualized by transferring seedlings to a water-agar plate containing bromocresol purple (Figure 4a). After 12 h of transfer to the bromocresol plate, the purple color around the rhizosphere of Al-treated wild-type plants changed to yellow compared with the control (0 μM AlCl₃ at pH 5.0). Correspondingly, the yellow regions around the rhizosphere of Al-treated plants were increased at 24 h and 48 h (Figure 4a). These results indicate that Al stress induces rhizosphere acidification.

Next, to evaluate the role of STOP1 and *SAUR55* in Al-induced H⁺ release into the rhizosphere, we performed a rhizosphere acidification assay in *STOP1*-KO and *saur55* (T-DNA insertion KO of *SAUR55*; Figure S3) under Al stress condition. No acidification around the rhizosphere of the *STOP1*-KO was observed (Figure 4b). By contrast, in the *STOP1*-complemented line, the rhizosphere acidification was fully recovered, similar to that of wild-type (Figure 4c). In the case of *saur55*, rhizosphere acidification was also substantially reduced than the wild-type (Figure 4b). Taken together, these results suggest that *SAUR55* is involved in rhizosphere acidification regulated by STOP1, which is possibly modulated by PM H⁺-ATPase under Al stress.

2.4 | Al and H⁺ tolerance of *saur55*

To examine the role of *SAUR55* expression in Al tolerance, we phenotyped the Al sensitivity of the *saur55* with other Al and/or H⁺ sensitive KO-mutants (i.e., both Al and H⁺-sensitive *STOP1*-KO, and Al sensitive *almt1* and *als3*; Sawaki et al., 2009). In the control solution (0 μM AlCl₃ at pH 5.5), all KO mutants grew similar to the wild-type. *saur55* showed a sensitive phenotype to Al compared with the wild-type under Al-stressed conditions (+Al at pH 5.5 or +Al at pH 5.0). At the same time, it was significantly more resistant than other Al-sensitive KO-mutants (*STOP1*-KO, *almt1*, and *als3*) (Figure 5a,b). Contrastingly, H⁺ rhizotoxicity (i.e., inhibition of root growth compared to pH 5.5) of *saur55* was slight at pH 5.0 and increased at pH 4.7 compared with the wild-type (Figure 5a,b). These results indicate that *SAUR55* expression contributes to both Al and H⁺ tolerance mechanisms in Arabidopsis.

To verify the correlation between *SAUR55* mediated H⁺ and malate exudation under Al stress in Arabidopsis, we studied malate release in the wild-type and *saur55* under control and Al stress. A significant reduction (25–30%; *P* < .05) of malate release was observed in *saur55* compared to the wild-type under Al stress (Figure 5c). These results suggest that *SAUR55*-mediated H⁺ exudation plays a role in root malate excretion in response to Al stress.

In addition, Al absorption in the root tip of *saur55* was visualized by morin staining, which is reported to easily form a fluorescent complex with cytosolic Al but hardly detected Al bound to the cell wall (Eticha et al., 2005). In the presence of Al (4 μM AlCl₃ at pH 5.0 for 24 h; Ikka et al., 2008), brighter fluorescence was observed in the roots of *saur55* but not in the wild-type (Figure 5d). The staining pattern of *saur55* was similar to that of the *almt1*, which showed strong fluorescence in the root elongation zone. This similarity further supported the possible association of *SAUR55*-dependent H⁺-release and *ALMT1*-dependent malate excretion for Al tolerance in Arabidopsis.

2.5 | Overexpression of *SAUR55* shows Al tolerance phenotype and increases rhizosphere acidification

To establish the relationship among *SAUR55*, rhizosphere acidification, and malate secretion for Al tolerance, *SAUR55* was overexpressed and complemented in wild-type and *STOP1*-KO respectively. More than 20 independent transgenic lines were obtained of which 3 lines were selected for further research. The overexpressing lines of *SAUR55* showed increased primary root length compared with the wild-type under Al-stressed conditions (+Al at pH 5.5 or +Al; pH 5.0). Furthermore, the H⁺ tolerance of *SAUR55*-overexpressed lines showed higher at pH 4.7 than at pH 5.0 (Figure 6a,b). In addition, to determine the H⁺-release ability of *SAUR55* into the rhizosphere under Al stress, a rhizosphere acidification assay for *SAUR55*-overexpressed lines (Figure 6c) was performed. As expected, the *SAUR55*-overexpressed lines showed higher rhizosphere acidification than the wild-type under Al stress (Figure 6d). Interestingly, it was also found that Al-activated malate excretion was enhanced by the *SAUR55*-overexpressed lines (Figure 6e). These results indicate that *SAUR55* has a significant role in enhancing Al-activated malate release by enhancing roots H⁺ exudation for Al tolerance.

On the other hand, the root growth and rhizosphere acidification of *SAUR55*-complemented lines introduced to the *STOP1*-KO were not observed under Al stress (Figure S4A and B). Likewise, the expression of *SAUR55* was not recovered in the *SAUR55*-complemented lines (Figure S4C) compared with the *SAUR55*-overexpressed lines (Figure 6c). In addition, complementation of *STOP2* (regulated by STOP1 and involved in both Al and low pH-tolerance mechanism; Kobayashi et al., 2014; Tokizawa et al., 2021) in *stop1* mutant could not rescue the expression of *SAUR55* under both Al- and low pH-stressed conditions (Figure S5). This indicates that *SAUR55* controls Al tolerance via STOP1 regulation.

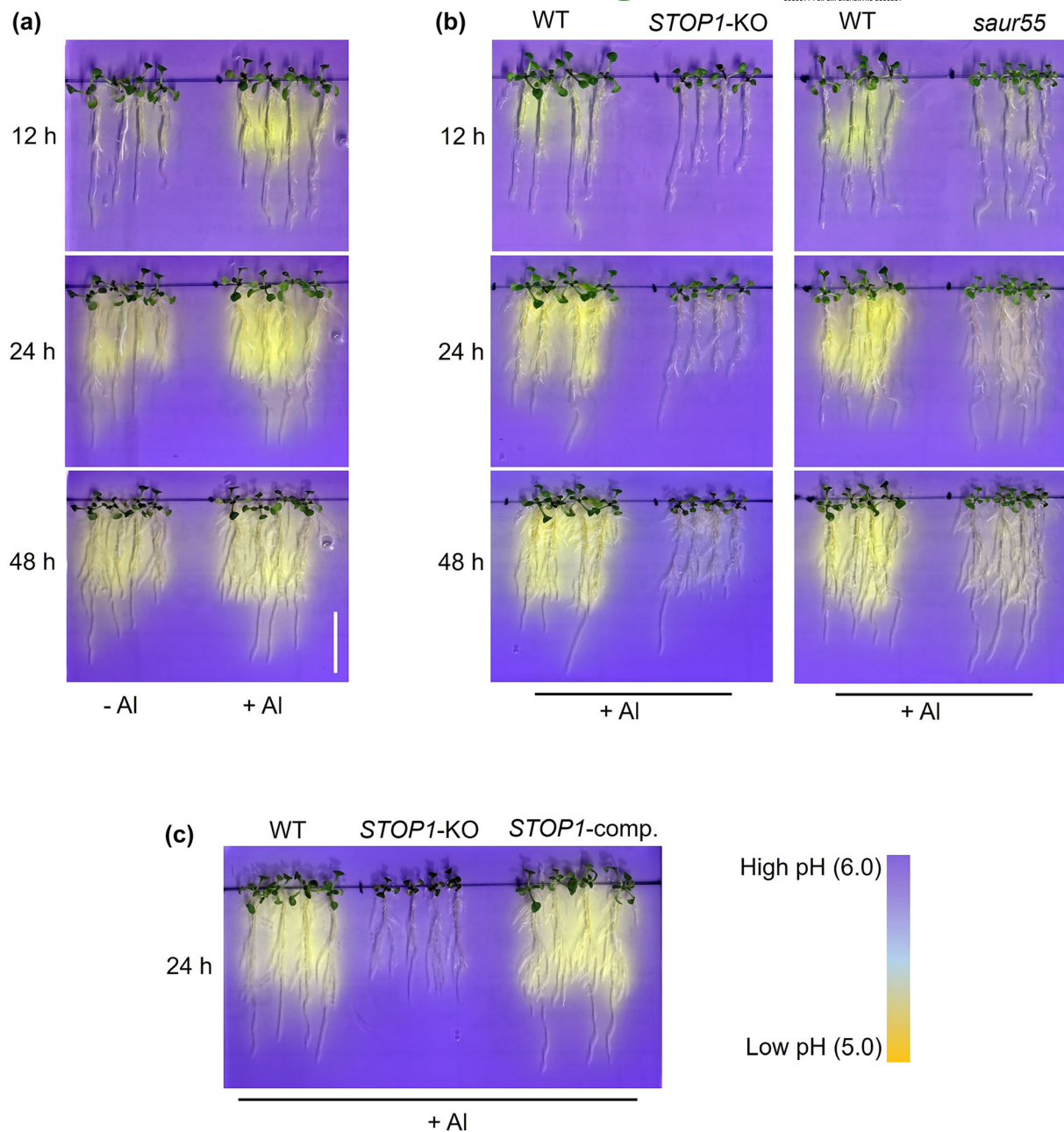


FIGURE 4 Involvement of *STOP1* and *SAUR55* in Al-induced rhizosphere acidification. (a) Induction of extensive rhizosphere acidification in wild-type (WT, Col-0) under Al stress. (b) Suppression of H^+ release into rhizosphere in *STOP1-KO* and *saur55* under Al stress. Ten-day-old seedlings were exposed to control ($0 \mu M AlCl_3$ at pH 5.0) and Al-containing ($10 \mu M AlCl_3$ at pH 5.0) solutions for 24 h. After 24 h of Al-treatment, the plants were transferred to the bromocresol purple (pH indicator dye) containing water-agar plate to visualize the rhizosphere acidification. Color changes were recorded at 12 h, 24 h, and 48 h. (c) Recovery of rhizosphere acidification in *STOP1*-complement (*STOP1-comp.*) after exposure to Al. Plants were pretreated with Al ($10 \mu M AlCl_3$ at pH 5.0) for 24 h and transferred to bromocresol purple-containing water-agar plate. Rhizosphere acidification was recorded at 24 h. Bar = 1 cm.

2.6 | *SAUR55* expression in natural variation of Arabidopsis

As in the overexpression lines, we quantified the expression of *SAUR55* in Arabidopsis accessions previously categorized as either Al-tolerant or Al-sensitive based on root phenotype and the expression of Al tolerance-related genes such as *ALMT1*, *ALS3* (*ALUMINUM SENSITIVE 3*; encodes a protein that reduces Al toxicity by

redistributing Al from sensitive tissues; Larsen et al., 2005), and *PGIP1* under Al stress (Agrahari et al., 2021; Kusunoki et al., 2017; Nakano et al., 2020; Sadhukhan, Agrahari et al., 2021). Comparison of the expression levels of *SAUR55* showed high expression in the Al-tolerant accessions (Col-0, Star-8, and Shigu-2) and low expression in the Al-sensitive accessions (Valsi-1, Ts-5, and Wei-0) (Figure 7a). In contrast, the genes for the nearest neighbors of *SAUR55* (i.e., *SAUR 74*, *76*, *77*, *78*, and *79*) did not differ in

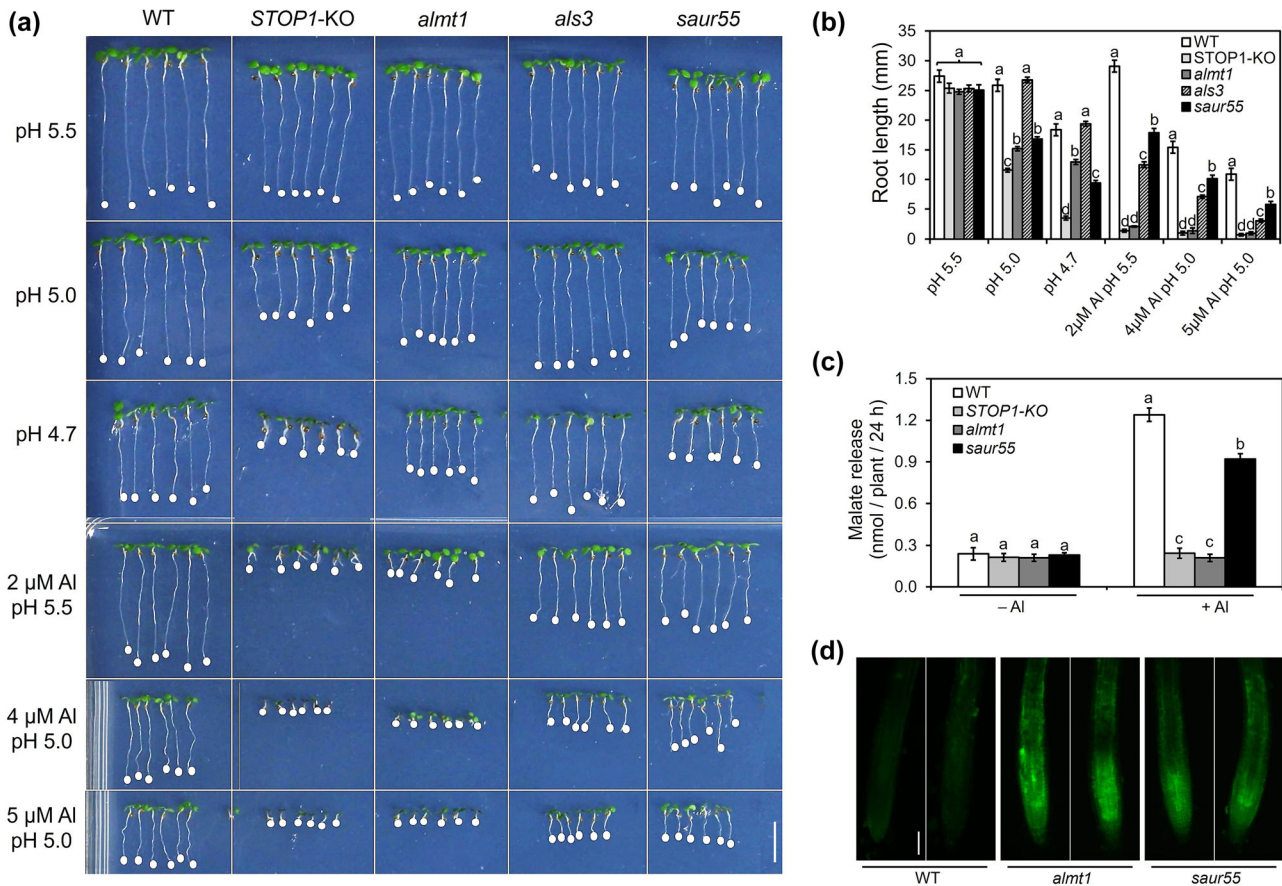


FIGURE 5 Comparison of root growth among T-DNA insertion knockout (KO) mutants under Al and H⁺ stress. (a) Growth response of *saur55* compared with that of wild-type (WT, Col-0), *STOP1*-KO, *almt1*, and *als3* grown under Al and H⁺ rhizotoxicity for 7 days. Bar = 1 cm. (b) The root length of each genotype treated with Al and H⁺ rhizotoxicity were presented as bar graphs. The average root length of the six longest seedlings (Kobayashi et al., 2013) among the 25 tested seedlings was presented with standard error (SE). Different letters in (B) indicate significant differences (least squared difference test, $P < .05$). (c) Malate excretion from roots of *saur55*. For the malate excretion assay, seedlings were treated with media containing -Al (0 μ M AlCl₃ at pH 5.0) or +Al (10 μ M AlCl₃ at pH 5.0) for 24 h. *STOP1*-KO and *almt1* were used as a positive control. Average values \pm SE ($n = 3$) are presented. Different letters on the error bars indicate significant differences at $P < .05$ (Tukey's test). (d) Morin staining of Al-treated roots of WT, *almt1*, and *saur55*. Seven-day-old seedlings were treated with Al (4 μ M AlCl₃ at pH 5.0) containing solution for 24 h. The fluorescence of morin was observed by a fluorescent microscope. Bar = 20 μ m.

expression levels in all those accessions. (Figure 7a). Furthermore, these accessions showed the differential pattern of rhizosphere acidification under Al stress (Figure 7b). Interestingly, accessions with higher proton release and higher expression levels of *SAUR55* also showed higher malate secretion (Figure 7c), which strongly indicates the relevance of *SAUR55* for Al-tolerance.

2.7 | Intracellular localization and interaction of the SAUR55 protein

Previous studies suggest that plasma membrane-localized SAURs physically interact with and inhibit protein phosphatases 2C.D (PP2C.D) to activate PM H⁺-ATPases (Ren et al., 2018). We, therefore, analyzed the intracellular localization of the SAUR55 protein by transient assay in onion (*Allium cepa* L.) epidermal cells using a GFP-fusion

protein. When the construct (i.e. 35S::SAUR55::GFP) was introduced to the epidermal cells by particle bombardment, the plasma membrane of cells fluoresced in green (Figure 8a). This localization pattern was similar to the 35S::AtPIP2A::mCherry (plasma membrane marker; Nelson et al., 2007). In addition, the plasmolysis of epidermal cells by .8 M mannitol further confirmed the localization of SAUR55 in the plasma membrane. Localization prediction also supported the results. We conducted a Kyte and Doolittle hydrophobic plot analysis based on the amino acid sequence of SAUR55 using the ProtScale program (Kyte & Doolittle, 1982; Hong et al., 2008). The analysis shows a hydrophobic pattern with distinct spikes in the SAUR55 protein (Figure 8b). In addition, the interaction of SAUR55 with PP2C.D2/D5/D6, key regulators of PM H⁺-ATPase (Ren et al., 2018), and PP2C.D5/D6/D7, involved in Al tolerance (Xie et al., 2023), was tested. Bimolecular fluorescence complementation (BiFC) assays showed that PP2C.D2 and PP2C.D5 physically interact with SAUR55 on the

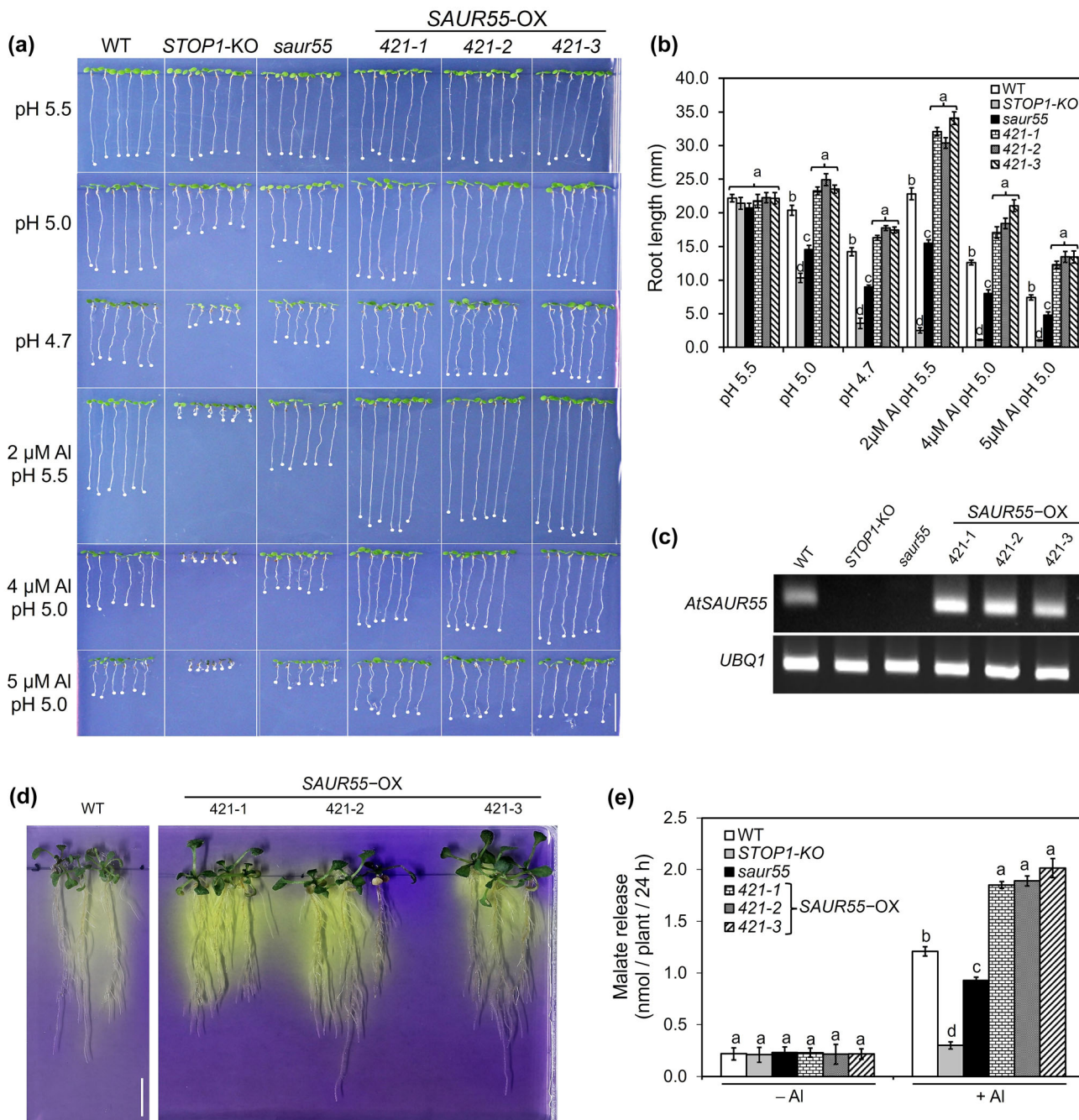


FIGURE 6 Al tolerance of Arabidopsis transgenic lines overexpressing SAUR55 (SAUR55-OX). (a) Growth response of SAUR55-OX lines compared with wild-type (WT, Col-0), STOP1-KO, and *saur55* under Al and H⁺ rhizotoxicity for 7 days. Bar = 1 cm. SAUR55 was introduced into the WT under the control of the SAUR55 native promoter. (b) Bar graph representing the root length of each genotype treated with Al and H⁺ rhizotoxicity. Among the 25 tested seedlings, the average root length of the 6 longest seedlings was presented with standard error (SE). Different letters in (b) indicate significant differences (least squared difference test, $P < .05$). (c) Semi-quantitative PCR bands showing SAUR55 expression in WT, STOP1-KO, *saur55*, and SAUR55-OX lines. The expression levels were measured from 10-day-old seedlings treated with Al (10 μ M AlCl₃ at pH 5.0) for 24 h. UBQ1 was used as an internal control. (d) Rhizosphere acidification of SAUR55-OX lines under Al stress. Ten days pre-grown seedlings were treated with Al for 24 h and transferred to bromocresol purple containing water-agar plate. Rhizosphere acidification was observed at 24 h. Bar = 1 cm. (e) Malate release in SAUR55-OX lines treated with -Al (0 μ M AlCl₃ at pH 5.0) or +Al (10 μ M AlCl₃ at pH 5.0) for 24 h. average values \pm SE ($n = 3$) are presented. Different letters on the error bars indicate significant differences at $P < .05$ (Tukey's test).

plasma membrane, whereas PP2C.D6 and PP2C.D7 showed no detectable interactions with SAUR55 (Figure 8c). These findings provide clear evidence that SAUR55 localizes in the plasma membrane

and physically interacts with PP2C.D2 and PP2C.D5, suggesting its involvement in the regulation of H⁺-ATPase in the plasma membrane under Al stress.

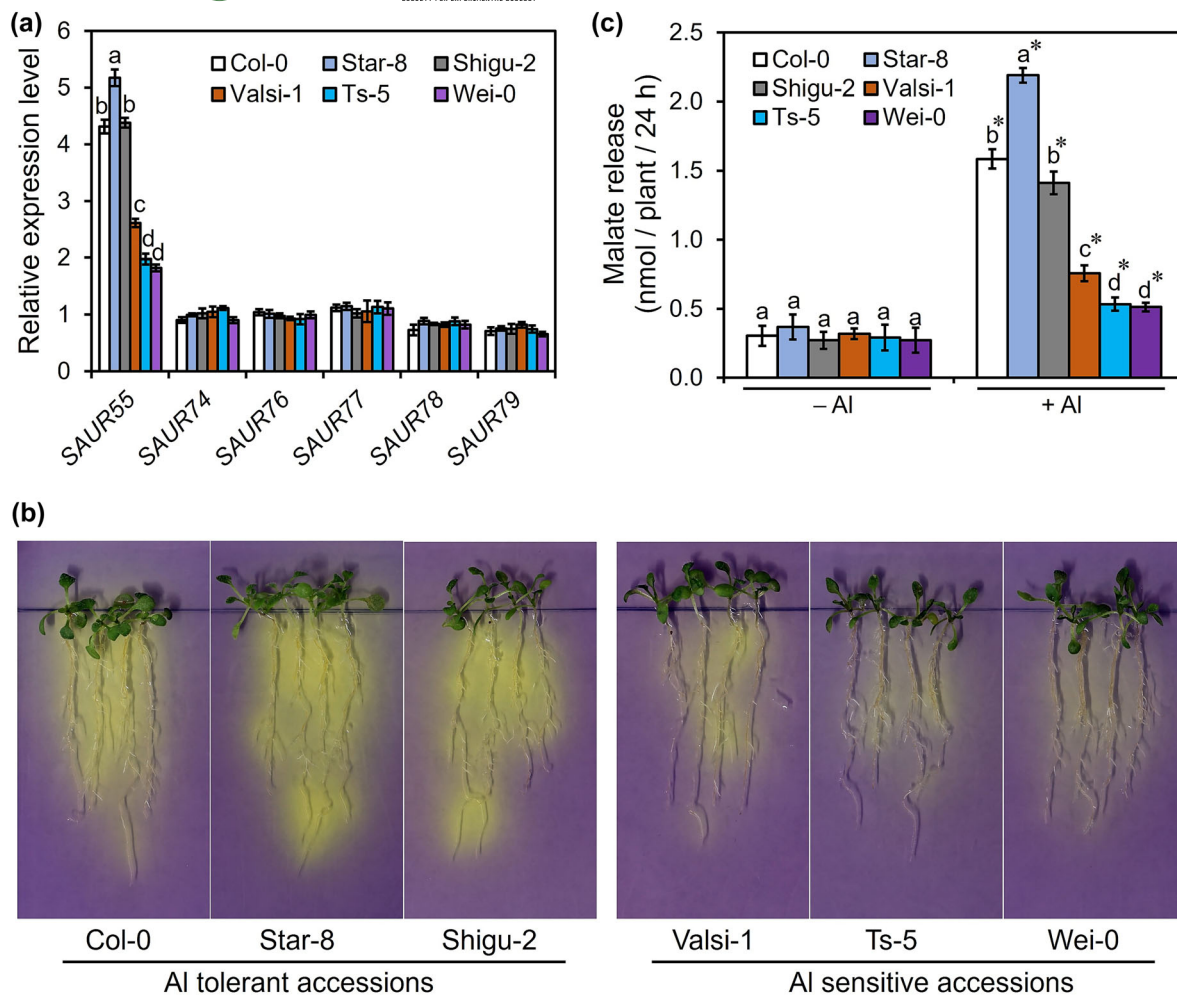


FIGURE 7 Natural variation associated with *SAUR55* in *Arabidopsis* accessions. (a) Relative expression levels of *SAUR55* along with its nearest neighbors (*SAUR* 74, 76, 77, 78, and 79) in roots of Al-tolerant (Col-0, Star-8, and Shigu-2; Kusunoki et al., 2017; Nakano et al., 2020) and -sensitive accessions (Valsi-1, Ts-5, and Wei-0; Kusunoki et al., 2017; Nakano et al., 2020) under Al (10 μM AlCl_3 at pH 5.0) treatment for 24 h. *UBQ1* was used as an internal control. The average values of three biological replicates are presented with standard error. Different letters on the error bars indicate significant differences at $P < .05$ (Tukey's test). (b) Rhizosphere acidification of Al-tolerant and -sensitive accessions under Al stress. Ten days pre-grown seedlings were treated with Al (10 μM AlCl_3 at pH 5.0) for 24 h and transferred to a bromocresol purple-containing water-agar plate. Rhizosphere acidification was observed at 24 h. Bar = 1 cm. (c) Malate release in Al-tolerant and -sensitive accessions treated with -Al (0 μM AlCl_3 at pH 5.0) or +Al (10 μM AlCl_3 at pH 5.0) for 24 h. average values \pm SE ($n = 3$) are presented. Different letters on the error bars indicate significant differences (Tukey's test; $P < .05$) within the -Al or +Al treatments, and asterisks above the +Al bars indicate significantly more malate exudation (Student's *t*-test; $P < .05$) than the control (-Al) treatment.

2.8 | *NtSTOP1* modulates H^+ release into the rhizosphere

To determine whether the STOP1-regulated Al-induced rhizosphere H^+ exudation is conserved across other plant species, the rhizosphere acidification assay was performed in tobacco. After 12 h of transfer to the water-agar plate containing bromocresol purple, Al-pretreated (10 μM AlCl_3 at pH 5.0 for 24 h) tobacco wild-type plants (*Nicotiana tabacum* var. Xianti) showed significant induction of rhizosphere acidification compared to the control (0 μM AlCl_3 at pH 5.0 for 24 h) (Figure 9a). In contrast, acidification around the rhizosphere of tobacco RNA interference (RNAi)-STOP1 knockdown (*NtSTOP1*-KD) lines was completely suppressed (Figure 9a). These findings suggest

that the STOP1-regulated rhizosphere H^+ exudation under Al stress is conserved in tobacco.

To further investigate whether the STOP-dependent regulation of *SAUR55* is conserved in tobacco, *SAUR55* orthologs were identified in tobacco by the BLAST-P program available on the NCBI database (<https://www.ncbi.nlm.nih.gov/search/>). Further, a phylogenetic tree with different evolutionary conserved amino acid motifs was constructed based on *SAUR55* of *Arabidopsis* and its related SAURs of tobacco by using the SALAD database (<https://salad.dna.affrc.go.jp/CGViewer/en/>; Zhou et al., 2020). Four putative orthologs (XP_016465095.1, XP_016489463.1, XP_016501814.1, and XP_016496213.1) of *SAUR55* having similar motifs were detected in tobacco (Figure 9b). Furthermore, our wet lab studies showed that

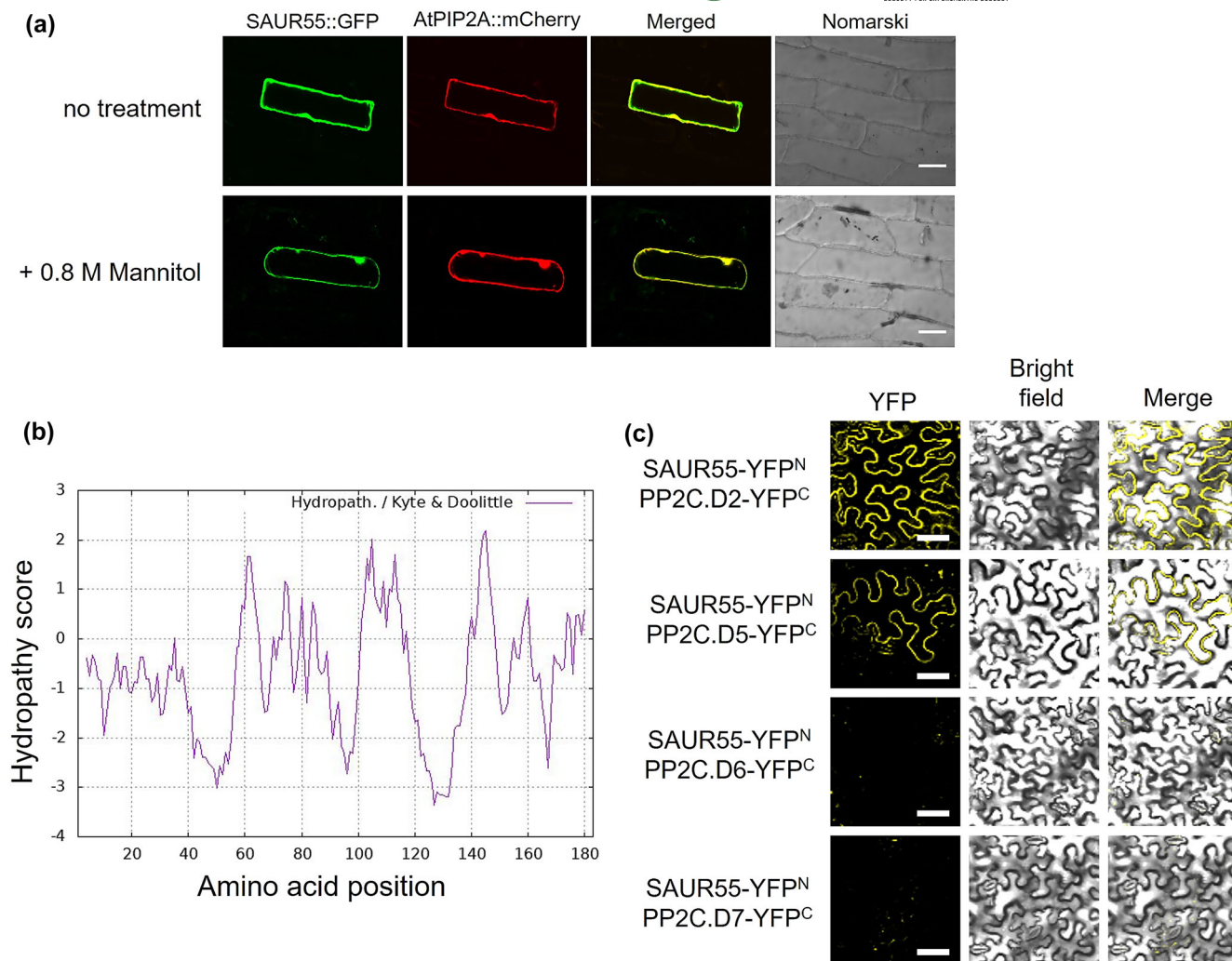


FIGURE 8 Plasma membrane-localized SAUR55 protein. (a) Localization of the SAUR55::GFP protein transiently expressed in onion epidermal cells. Vectors containing 35S::SAUR55::GFP and 35S::AtPIP2A::mCherry (plasma membrane marker; Nelson et al., 2007) were introduced by particle bombardment. Fluorescent images of GFP (left), mCherry (middle left), and merged images (middle right). Plasmolysis of onion epidermal cells with .8 M mannitol confirmed plasma membrane localization of SAUR55 (bottom). Bars = 100 μm . (b) Hydropathy plot of the SAUR55 protein. Kyte and Doolittle hydropathic plot analysis was performed using the ProtScale program (Kyte & Doolittle, 1982) based on the amino acid sequence of SAUR55 to predict transmembrane domains. Peaks with scores greater than 1.8 indicate a possible transmembrane region. (c) Bimolecular fluorescence complementation (BiFC) visualization of the interaction of SAUR55 with PP2C-D2, D5, D6, and D7 using agrobacterium-mediated transient transformation of *Nicotiana benthamiana*. Fluorescent signal was detected when the leaves were infiltrated with SAUR55-YFP^N and PP2C.D2-YFP^C or PP2C.D5-YFP^C. Bars = 50 μm .

two of them (XP_016465095.1 and XP_016489463.1) were inducible by AI stress (Figure 9c) and were repressed in the *NtSTOP1*-KD lines (Figure 9d). These results showed that the AI-inducible tobacco SAUR55 orthologs (XP_016465095.1 and XP_016489463.1) are regulated by *NtSTOP1*. Taken together, these results indicate that the *STOP1*-regulated SAUR mechanism for AI tolerance is conserved in tobacco.

2.9 | The PM H⁺-ATPase genes in response to AI

As reported previously (Ohno et al., 2003; Shen et al., 2005), the plant treated with vanadate (VA), an inhibitor of PM H⁺-ATPase,

suppressed the AI-induced secretion of OAs such as malate (Figure 10a). This suppression increased with increasing VA concentration, indicating a strong relationship between PM H⁺-ATPase and malate secretion under AI stress. To determine whether *STOP1* transcriptional regulation contributes to the induction of the PM H⁺-ATPase gene under AI stress, we analyzed the expression of PM H⁺-ATPase encoding genes (*AHA1*–*AHA11*; Palmgren, 2001) under AI stress (Figure 10b). *AHA1*, *AHA2*, and *AHA7* showed significant induction under AI stress, while the transcription levels of most PM H⁺-ATPase gene family members remained unchanged. Among these three AI inducible genes, the expression level of *AHA2*, a major PM H⁺-ATPase isoform expressed in *Arabidopsis* roots (Harper et al., 1990), was strongly induced by AI and significantly suppressed

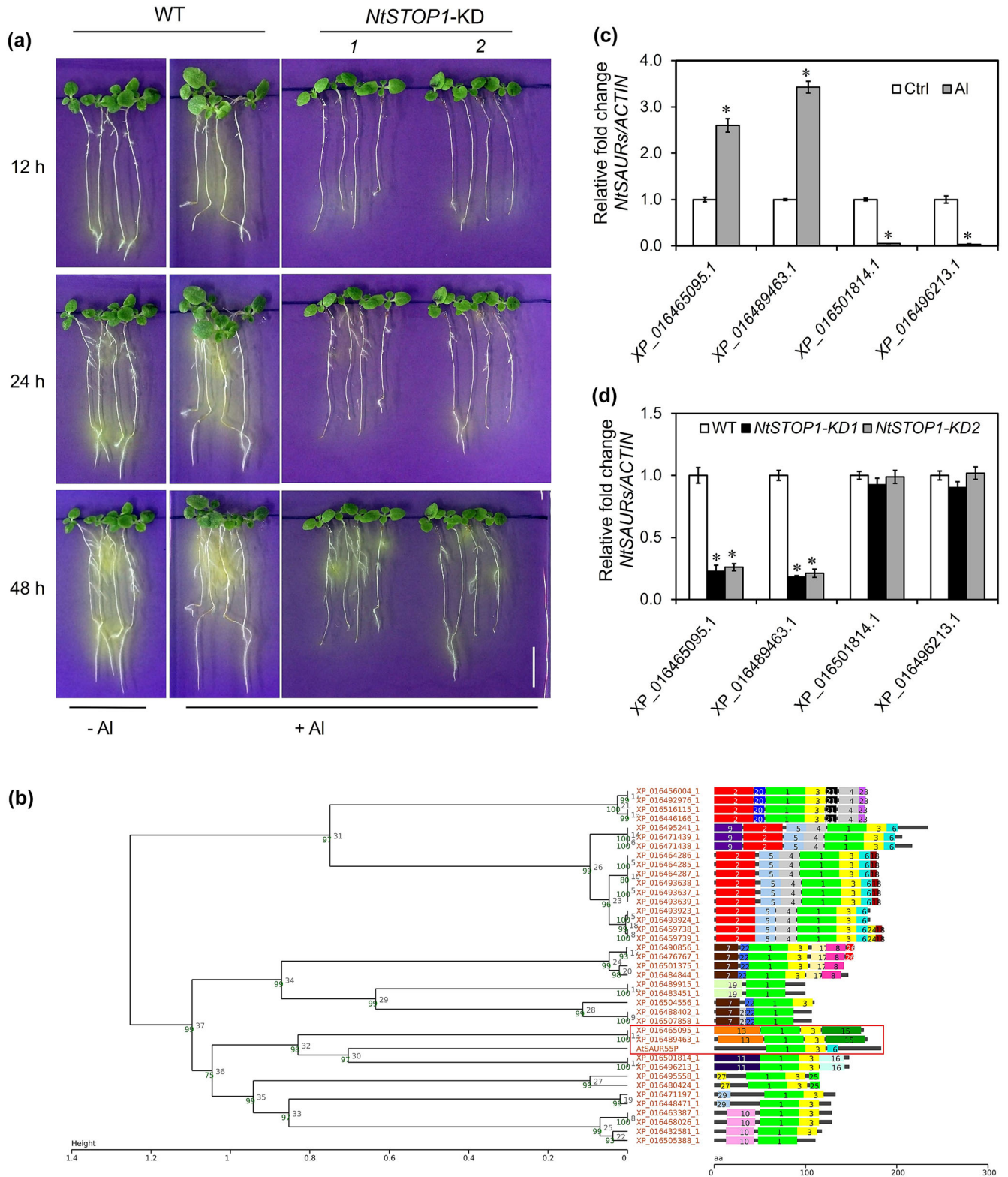


FIGURE 9 Legend on next page.

FIGURE 9 *NtSTOP1* regulates Al-induced H^+ release into rhizosphere in tobacco. (a) Induction of extensive rhizosphere acidification in wild-type (WT, *Nicotiana tabacum* var. Xianti) and RNAi suppressing lines of *NtSTOP1*-knockdown (*NtSTOP1*-KD) under Al stress. Ten-day-old seedlings were exposed to a nutrient solution containing $-Al$ ($0 \mu M AlCl_3$ at pH 5.0) or $+Al$ ($10 \mu M AlCl_3$ at pH 5.0) for 24 h. After 24 h, the plants were transferred to bromocresol purple-containing water-agar plate. Rhizosphere acidification was observed at 12 h, 24 h, and 48 h. Bar = 1 cm. (b) A phylogenetic tree showing conserved amino acid motifs of AtSAUR55 in putative SAURs of tobacco. The phylogram was constructed based on the SAUR55 protein sequence using the SALAD database. Each motif is assigned a sequence number and color within the 'high percent similarity' protein group, and the same color box represents the same extracted motif. The red color box indicates that the tobacco SAURs exhibit the highest structural homology with AtSAUR55. (c) Expression levels of four putative *NtSAURs* (*XP_016465095.1*; *XP_016489463.1*; *XP_016501814.1* and *XP_016496213.1*) closely related to SAUR55 in roots of tobacco under control and Al stress. (d) Expression levels of Al-inducible putative *NtSAURs* (*XP_016465095.1* and *XP_016489463.1*) in the roots of WT and *NtSTOP1*-KD lines under Al stress. Tobacco seedlings were grown for 10 days and then treated with $-Al$ ($0 \mu M AlCl_3$ at pH 5.0) or $+Al$ ($10 \mu M AlCl_3$ at pH 5.0) for 24 h. Average values of three biological replicates were presented with standard errors. *ACTIN* was used as an internal control. The asterisk indicates a significant difference as determined by Student's *t*-test ($P < .05$).

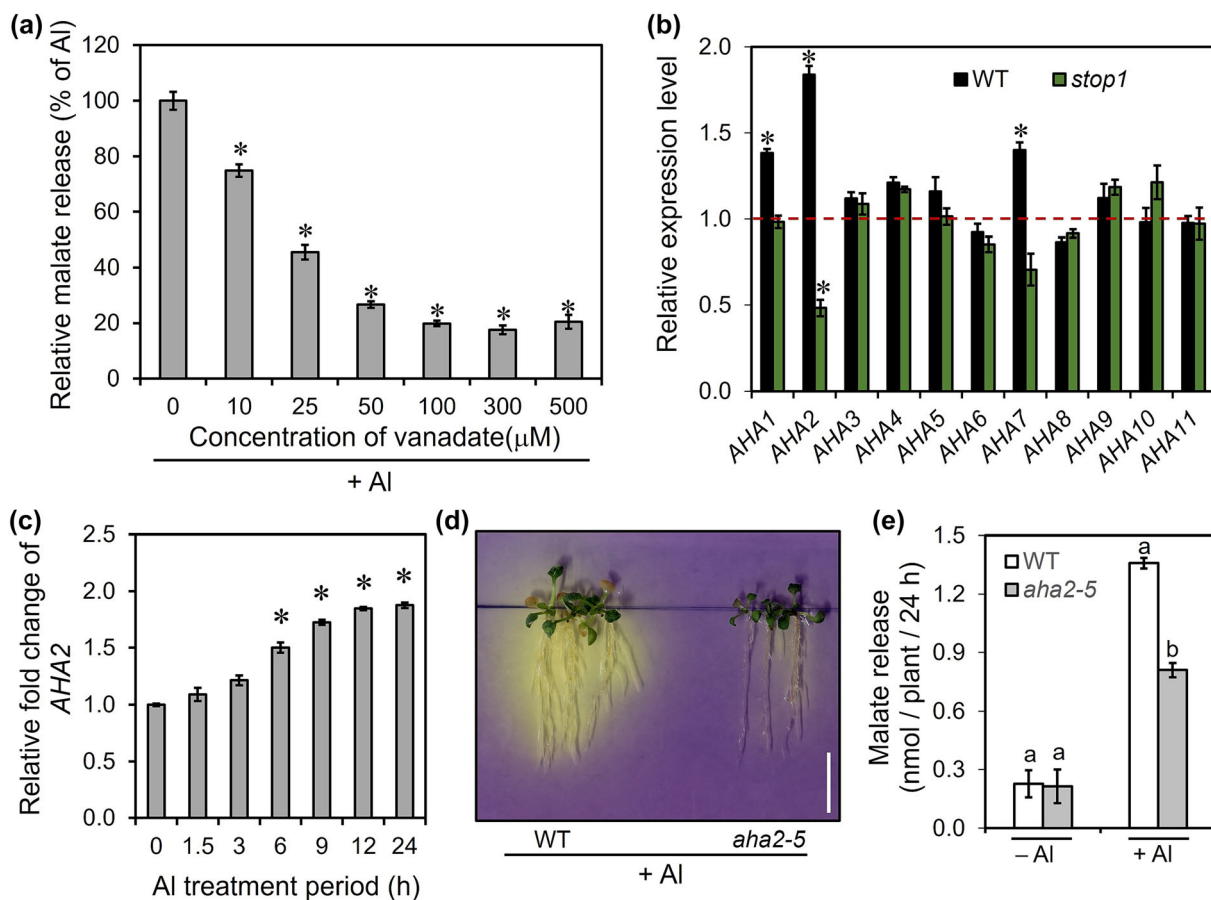


FIGURE 10 Involvement of AHA2 in rhizosphere acidification and malate secretion under Al. (a) Effects of vanadate on malate release in Al-treated Arabidopsis roots. Arabidopsis (Col-0) seedlings were incubated in an Al-containing ($10 \mu M AlCl_3$ at pH 5.0) media for 24 h in the presence of various concentrations of vanadate. (b) Expression of PM H^+ -ATPase gene family members (AHA1-AHA11) in wild type (WT, Col-0) and STOP1 mutant (*stop1*) under control ($-Al$) and Al stress treatment for 24 h are shown. The expression data in the root was obtained from our previous microarray data (Sawaki et al., 2009). The dotted line represents the ratio of gene expression with Al to that without Al. (c) Expression profiling of AHA2 in the root of Arabidopsis in response to Al ($10 \mu M AlCl_3$ at pH 5.0) for different time periods. The roots were excised from 10-day-old 100 seedlings of Arabidopsis (WT, Col-0) exposed to different treatments. Relative fold change was calculated as the ratio of gene expression in growth media with Al to that without Al. *UBQ1* was used as an internal control. The average data of three biological replicates are presented with standard errors. Asterisks indicate significant differences at $P < .05$ (Student's *t*-test). (d) Rhizosphere acidification in WT and *aha2-5* under Al stress. Ten-day pre-grown seedlings were treated with Al ($10 \mu M AlCl_3$ at pH 5.0) for 24 h and transferred to a bromocresol purple-containing water-agar plate. Rhizosphere acidification was observed at 24 h. Bar = 1 cm. (e) Malate excretion from roots of WT and *aha2-5*. For the malate excretion assay, seedlings were treated with media containing $-Al$ ($0 \mu M AlCl_3$ at pH 5.0) or $+Al$ ($10 \mu M AlCl_3$ at pH 5.0) for 24 h. average values \pm SE ($n = 3$) are presented. Different letters on the error bars indicate significant differences (Tukey's test; $P < .05$) within the $-Al$ or $+Al^{3+}$ treatments.

in the *stop1* mutant (Figure 10b). Further time-course analysis showed that *AHA2* transcripts in the wild-type were gradually induced under Al stress (Figure 10c). We, therefore, used an *AHA2*-KO mutant (*aha2-5*; Haruta et al., 2010) to analyze root rhizosphere acidification and malate release. Interestingly, we found a significant reduction of rhizosphere acidification and malate release in the *aha2-5* than the wild-type as well as *saur55* (Figure 10d,e). Taken together these data strongly indicate the involvement of *AHA2* in Al tolerance.

3 | DISCUSSION

H⁺ transport of the PM H⁺-ATPases plays a crucial role in ion transport of the plasma membrane because it provides an electrochemical gradient at the plasma membrane (Falhof et al., 2016; Siao et al., 2020; Yu et al., 2016). Recent studies revealed that SAURs are positive regulators of the PM H⁺-ATPases by inhibiting PP2C.D family that inactivates PM H⁺-ATPase (e.g., *AHA2*; Spartz et al., 2014; Ren et al., 2018; Wong et al., 2021). The SAURs in Arabidopsis, which consist of 79 members, found that most of the SAURs are responsive to growth hormones (such as IAA and ABA) and are highly expressed in growing parts of plants to modulate PM H⁺-ATPase activity (Ren & Gray, 2015). By contrast, different regulation was reported in several SAURs such as -P inducible expression of *SAUR19*, which is involved in the signal transduction of P-deficiency (Młodzinska-Michta, 2022). In this study, we identified that one of the SAURs, i.e., *SAUR55* is responsive to Al (Figure 2b,c), while it showed typical characteristics of SAURs regulating PM H⁺-ATPases. For example, GFP-tagged *SAUR55* localized on the plasma membrane (Figure 8), and the expression levels correlated with H⁺ release from the root cells (Figure 4b and Figure 6d). The T-DNA insertion mutant *saur55* was significantly more sensitive to Al and H⁺ stress than the wild-type (Figure 5). *SAUR55* expression was found to be inducible under low pH however, the expression level is even less than that of Al stress (Figure S6 and Figure 2a). It revealed that *SAUR55* has unique roles in Al response than other SAURs and controls H⁺ and Al tolerance of Arabidopsis. Stress-responsiveness of plant architecture is determined by the expression level of the genes, which varies among natural accessions. Recently, Wang et al. (2019) showed *SAUR26* cluster genes heat tolerance by quantifying their expression in Arabidopsis accessions that have higher thermo-responsiveness. Furthermore, recent studies on the differential expression patterns of Al tolerance genes, including *ALMT1*, between Al-tolerant and sensitive accessions, have shown to be very useful in finding the relationship between Al-tolerant genes and tolerance levels (Kusunoki et al., 2017; Nakano et al., 2020). Similarly, the present study also reveals an association between the variation in the expression level of *SAUR55* and Al tolerance (Figure 7).

Al tolerance of *saur55*, *SAUR55*-OX, and natural accessions could be explained by the level of malate excretion, which is one of the major Al tolerance mechanisms in Arabidopsis identified by an Al tolerance GWAS (Nakano et al., 2020). Functions of *SAUR55* in the rhizosphere acidification (Figures 4b and 6d) and malate excretion (Figures 5c and 6e) were similar to those of *AHA2* under Al stress

(Figure 10). In addition, as for *AHA2* being considered downstream of *STOP1* (Figure 10b), the Cistrome database (<http://neomorph.salk.edu/dap%20web/pages/>) shows *STOP1*-binding capacity in the promoter region of *AHA2* (Figure S8). Conversely, Zhang et al. (2019) demonstrated that the *aha2* mutant displayed sensitivity to Al stress, indicating the involvement of *AHA2* in the Al tolerance mechanism, while Spartz et al. (2014) revealed that SAUR proteins could regulate *AHA2* by inhibiting PP2C.D phosphatase, impacting plant growth and development. On the other hand, Xie et al. (2023) recently reported that root growth and Al-induced malate excretion were higher and lower in *Atpp2c.d5d6d7* and *aha2* mutants, respectively. Collectively, these findings support the notion that Al tolerance is mediated through the H⁺-ATPase activation system regulated by *SAUR55* via interaction with PP2C.D2 and PP2C.D5 (Figure 8c), which is controlled by *STOP1* and cooperates with malate secretion under Al stress (Figure 11).

Co-expression gene network includes a gene for another possible protein that is involved in the regulation of malate excretion by *AtALMT1* (Figure 1). The molecular function of *SIF1* has not been characterized yet, but a homolog *SIF2* (malectin-like receptor-like kinase STRESS INDUCED FACTOR 2) was reported that is critical for activation of a malate transporter *SLAC1* in the stomatal guard cells in bacterial response (Chan et al., 2020). *SIF1* might be involved in the Al activation of *ALMT1*, while further research will be needed to investigate this possibility. By contrast, the H⁺-sensitivity of *saur55* could be explained by the lower activity of H⁺-release that induces acidification of the cytosol (Sadhukhan, Kobayashi, et al., 2021). Furthermore, the H⁺-sensitivity of *saur55* could also be explained by the association of other genes belonging to the co-expression genes network of *AtALMT1*. K⁺ transport by *HAK5* requires an electrochemical generated by the H⁺-transport of PM H⁺-ATPases, while higher K⁺ levels in the cytosol contribute to maintaining cytosol pH above 7 (Walker et al., 1998). Taken together, *saur55* may become susceptible to H⁺ toxicity due to a lower capacity to maintain cytosol pH. The co-expression network contains other proteins that were characterized as the H⁺-tolerance genes, such as *STOP2* (Kobayashi et al., 2014) and *PGIP1* (stabilizing cell wall pectin at low pH; Kobayashi et al., 2014). Our findings *SAUR55* further provide stress physiological importance of the *STOP1* regulating system for Al and H⁺-tolerance.

While genome-wide studies have been limited (i.e., transcriptome studies using mutants), the conservation of *STOP1*-regulated Al tolerance has been reported in various plants. Comparison of suppressed genes in mutants of *STOP1*-like proteins in Arabidopsis (Sawaki et al., 2009), tobacco (Ito et al., 2019), and rice (Yamaji et al., 2009) identified several common Al tolerance genes, including genes for organic acid (OA) transporters. RNAi suppression of *STOP1*-protein in pigeon peas (Daspute et al., 2018) and eucalyptus (Sawaki et al., 2014) confirmed the regulation of Al-tolerance *MATE* expression by *STOP1* orthologs. These studies revealed the transcriptional regulation of OA transporters by *STOP1*-like proteins in various plants. In contrast, the co-excretion of H⁺ and citrate has been reported in soybean (Shen et al., 2005), carrot (Ohno et al., 2003, 2004), and white lupin (Neumann et al., 1999; Tomasi et al., 2009),

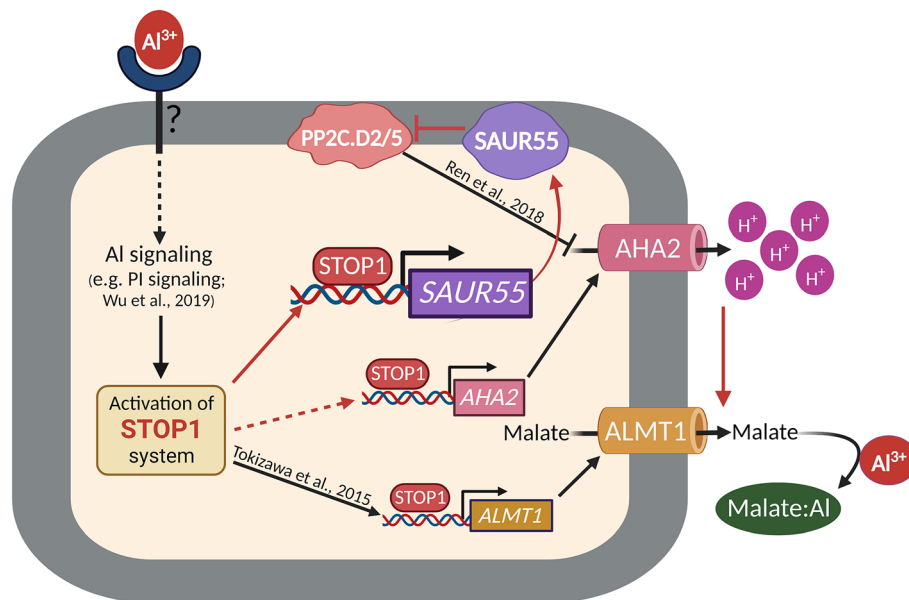


FIGURE 11 Schematic representation of *SAUR55* regulation by *STOP1* in relation to Al tolerance. Al stimulates the phosphoinositide (PI)-signal transduction pathways (Wu et al., 2019), which activate the *STOP1*-system for transcriptional regulation of the major Al tolerance gene, such as *ALMT1* through promoter binding (Tokizawa et al., 2015). This model represents the molecular mechanism that includes the involvement of a new player i.e., *SAUR55* for Al-induced H^+ release. *SAUR55* is inducible by Al and directly regulated by *STOP1* through promoter binding. *SAUR55* is involved in the positive regulation of the plasma membrane (PM) H^+ -ATPase pump by inhibiting PP2C.D2/5 phosphatases, reported as negative regulators of PM H^+ -ATPase (*AHA2*; Ren et al., 2018). Together, this model explains Al-induce the expression of *SAUR55* through *STOP1*, which modulates *AHA2* (*AHA2* promoter have *STOP1*-binding capacity determined by the Cistrome database (Figure S8), and its expression is suppressed in *stop1*), for proton/malate co-secretion for Al tolerance in Arabidopsis. The black arrow represents previous findings, and the red arrow represents newly identified regulations in this study.

which is associated with the activation of PM H^+ -ATPase. In this study, we found that H^+ -excretion in Arabidopsis showed *STOP1*-dependent transcriptional regulation (Figure 4b,c). While tobacco possesses *STOP1*/*MATE*-dependent Al-inducible citrate excretion but not malate excretion via *ALMT1* (Ohyama et al., 2013), it showed a substantial reduction of rhizosphere acidification (Figure 9a) and expression of *SAUR55* putative orthologs in transgenic tobacco where *NtSTOP1* was suppressed by RNAi (Figure 9d). These findings suggest that the coregulation of genes for OA transporters and SAUR by *STOP1*-like proteins contributes to enhancing malate excretion in Arabidopsis and may be involved in citrate excretion in other plant species, including tobacco, under Al-stressed conditions. However, characterizing the role of *NtSAURs* in Al-triggered PM H^+ -ATPase activity and citrate excretion is a future research endeavor.

In Arabidopsis, an F-box protein *RAE1* (Zhang et al., 2019) negatively regulates *STOP1* by modulating the stability of *STOP1* under Al-stress-free conditions. The *STOP1*/*RAE1* forms negative feedback of *STOP1* by positive regulation of *RAE1* expression by *STOP1*. Such negative feedback would be originated from unknown common ancestor of higher plants and bryophytes because Rico-Reséndiz et al. (2020) reported that *Marchantia* upregulated *ALMT1* and *RAE1* orthologs under -P stress, which is one of the inducers of *STOP1* regulating system in Arabidopsis (Balzergue et al., 2017; Zhang et al., 2019). On the other hand, recent studies of *SAURs* revealed that an increasing copy number of *SAURs* has occurred in higher plants because bryophyte carries fewer copies of *SAURs* (5 copies in *Marchantia*

polymorpha) than in higher plants (42 copies in *Ginkgo biloba*; 58 copies in *Oryza sativa*; and 79 copies in Arabidopsis) (Zhang et al., 2021). This gene amplification in higher plants allows tissue/cell and stress-specific regulation of *SAURs*, which can contribute to precisely regulate PM H^+ -ATPase activity (Stortenbeker & Bemer, 2019). For example, heat (*SAUR26* of IAA inducible cluster; Wang et al., 2021), light (*SAUR16* and *SAUR50*; Dong et al., 2019), and cell-specific (*SAUR56* and *SAUR60*; Wong et al., 2021) expression of several *SAURs* are identified in Arabidopsis (Figure S7). Our findings revealed that a specific *SAUR* is transcriptionally controlled by *STOP1* under Al stress, at least, in Arabidopsis and tobacco. A tobacco ortholog of *SAUR55* showed the highest homology of amino acid sequence with Arabidopsis *SAUR55* (Figure 9b). In addition, tobacco ortholog showed the same expression profile that was observed in Arabidopsis *SAUR55*, including inducible by Al and suppressed in the *stop1* genotype (Figure 9c,d). It suggests that both the protein and the promoter of *SAUR55* in Arabidopsis and tobacco ortholog may share a common origin. Further functional characterization of *SAURs* in different higher plants could answer this question.

4 | CONCLUSION

In this study, we have successfully identified a distinct Al-inducible member of the *SAUR* family, specifically *SAUR55*, in Arabidopsis, through a comprehensive transcriptome analysis. Our data provides

compelling evidence that STOP1 plays a pivotal role in activating SAUR55's transcription, as it directly binds to its promoter in response to Al stress. Furthermore, we have elucidated the subcellular localization of SAUR55 within the plasma membrane, affirming its involvement in rhizosphere acidification when exposed to Al stress. We have also confirmed the interaction of SAUR55 with PP2C.D2 and D5, which are negative regulators of PM H⁺-ATPase 2. These collective findings strongly suggest the potential role of SAUR55 in regulating PM H⁺-ATPase 2 activation under Al stress. Moreover, our study emphasizes the critical role played by STOP-regulated SAUR55 in enhancing the Al exclusion mechanism. This enhancement is achieved through facilitated malate secretion, potentially by modulating PM H⁺-ATPase 2, thus improving the plant's response to Al toxicity.

5 | MATERIALS AND METHODS

5.1 | Plant materials

Arabidopsis accession Col-0 was obtained from the RIKEN Bioresearch Research Center (RIKEN BRC; Tsukuba, Japan). T-DNA insertion mutants were obtained from the Arabidopsis Biological Resource Center (Columbus, OH, USA) and The Nottingham Arabidopsis Stock Center (Nottingham, UK). A single seed descent procedure was used to multiply the procured seeds prior to experimental usage. In this work, the T-DNA insertion KO mutants were *STOP1*-KO (At1g34370, SALK_114108; Sawaki et al., 2009), *almt1* (At1g08430, SALK_134416; Sawaki et al., 2009), *aha2-5* (At4g30190, SALK_022010; Haruta et al., 2010) and *saur55* (At5g50760, SALK_065086). Homozygosity of the *saur55* was verified using primers from the SALK database (<http://signal.salk.edu/tdnaprimers.2.html>) according to their protocols. Primer sequences are listed in Table S1. The Arabidopsis accessions (Star-8, Shigu-2, Valsi-1, Ts-5, and Wei-0), *stop1* mutant, *STOP1*- and 35S::*STOP2*-complemented lines were identical to that used in our previous study (Agrahari et al., 2021; Kobayashi et al., 2014; Kusunoki et al., 2017; Nakano et al., 2020). For tobacco (*N. tabacum* var. Xianti), seeds of the wild-type and an RNAi-suppressing line of *NtSTOP1*-KD were identical to that used in our previous study (Ito et al., 2019; Ohyama et al., 2013). All growth experiments were conducted at least three times and confirmed reproducibility.

5.2 | Growth conditions

The Al-tolerant root growth test was performed with the method described by Kobayashi et al. (2007). Briefly, Arabidopsis seedlings were grown hydroponically at 22 °C under a 12 h day/night cycle (PPFD; 40 μmol m⁻² s⁻¹) in 2% modified MGRL-nutrients (CaCl₂ was increased to give a final concentration of 200 μM to support root growth, Pi was removed to enhance Al toxicity) for 7 days. The nutrient solutions were renewed every 2 days. The plants were photographed at 7 days, and the primary root lengths were measured using

LIA32 software (<https://www.agr.nagoya-u.ac.jp/~shinkan/LIA32/index-e.html>).

For RNA isolation, approximately 100 seedlings were pre-grown for 10 days in stress-free conditions (0 μM AlCl₃ at pH 5.6, 2% MGRL containing 200 μM CaCl₂) in a floating plastic mesh (Toda et al., 1999). Subsequently, the seedlings were transferred to the Al (modified 2% MGRL without Pi, 10 μM AlCl₃, pH 5.0) as well as low pH, IAA, and ABA stress solutions, as previously described (Kobayashi et al., 2013; Sawaki et al., 2009). Plant tissues were harvested without touching the plants to avoid wounding. The root tissues were immediately frozen in liquid nitrogen and stored at -80 °C after harvesting.

5.3 | Bioinformatics of SAUR55

The homology of SAUR55 with other members of the SAUR family was analyzed by constructing a phylogenetic tree using protein sequences retrieved from the TAIR database (<https://www.arabidopsis.org/>) by the neighbor-joining method using MEGA 6.0 (Tamura et al., 2013). The signal response of SAURs was profiled using publicly available transcriptome data. Al response and STOP1 regulated expression were profiled by microarray data obtained by Sawaki et al. (2009). Competitive microarray data of three biologically independent replications under control (0 μM AlCl₃ at pH 5.0 for 24 h) versus Al (10 μM AlCl₃ at pH 5.0 for 24 h) and *stop1* versus the wild-type in Al (10 μM AlCl₃ at pH 5.0 for 24 h) were retrieved through the ArrayExpress database (<http://www.ebi.ac.uk/microarray-as/ae/>) with accession code E-MEXP-1908. Relative fold changes of the SAURs family in the wild-type and *stop1* under Al conditions (10 μM AlCl₃ at pH 5.0 for 24 h) were compared with control conditions (0 μM AlCl₃ at pH 5.0 for 24 h). The IAA and ABA response of SAURs was profiled using publicly available microarray data from the EXPath database (<http://expath.itps.ncku.edu.tw/>). The co-expression genes network was created using the ATTED-II v11 database (<https://atted.jp/>; Obayashi et al., 2022).

5.4 | RNA extraction and quantitative RT-PCR analyses

Sepasol-RNA I Super G (Nacalai Tesque, Kyoto, Japan) was used to extract total RNA according to the manufacturer's instructions. The RNA quality was analyzed using the A260/A280 ratio on a NanoVue Plus spectrophotometer (Biochrom, Holliston, USA). Total RNA was reverse transcribed using ReverTra Ace (Toyobo, Osaka, Japan) according to the manufacturer's instructions before being used in qRT-PCR. qRT-PCR was carried out using THUNDERBIRD SYBR qPCR Mix (Toyobo, Osaka, Japan) with a Dice Real Time System II MRQ thermal cycler (Takara Bio, Otsu, Japan) according to the manufacturer's instructions. Briefly, all quantifications were carried out based on the qRT-PCR standard curve method following the MIQE guidelines of Bustin et al. (2009), as described by Kobayashi et al. (2014). The expression level of *Ubiquitin 1* (*UBQ1*; AT3G52590; for



Arabidopsis; Kobayashi et al., 2014) and *ACTIN* (for tobacco; Ohya et al., 2013) were used as internal controls. We checked the invariant expression of *UBQ1* and *ACTIN* for all experimental conditions in the lines used in this study. The primers used for the analyses are listed in Table S1.

5.5 | In vitro protein-dsDNA binding assay

An amplified luminescent proximity homogeneous assay (AlphaScreen™, PerkinElmer, Waltham, MA, USA) with the EnSpire Multimode Plate Reader (PerkinElmer, Waltham, MA, USA), was used to investigate STOP1 binding to double-stranded synthetic promoter fragments as described by Enomoto et al. (2019). Competition assays using non-biotinylated probes (450 nM) were performed by following the manufacturer's instructions. *SAUR55* probes were designed around the putative STOP1-binding region i.e. -1,480 to -1,441 bp upstream from the start codon, according to Plant Cistrome Database (<http://neomorph.salk.edu/dap%20web/pages/>). The control probes (CIS-D, a known STOP1-binding site on the *ALMT1* promoter, was used as the positive control, and the *ALMT1* promoter's CIS-A region, where STOP1 does not bind, was used as a negative control) used were the same as described by Tokizawa et al. (2015). Probe sequences are listed in Table S1.

5.6 | Generation of transgenic hairy roots

Transgenic hairy roots were generated from the Arabidopsis stems according to the method of Nakano et al. (2020). Cut stems of Arabidopsis were infected with *Agrobacterium rhizogenes* containing *SAUR55* promoter::*GUS* constructs. Infected stems were subsequently grown in a half-strength MS medium (Murashige & Skoog, 1962) containing 1% sucrose and agar, along with .2 mM of acetosyringone. After three days of culture, the stems were transferred to the selection medium used by Nakano et al. (2020) with a little modification of kanamycin B as an antibiotic. Until hairy root formation, the selection medium was renewed every week. The generated hairy roots were used to evaluate *GUS* expression. Approximately 20 to 30 hairy roots were treated with Al-containing solution (modified 2% MGRL without Pi, 10 μM AlCl₃ at pH 5.0) for 24 h and then frozen in liquid nitrogen. Total RNA extraction, reverse transcription, and qRT-PCR were performed as described above. *GUS* expression levels were measured using specific primer pairs (Table S1). The expression level of *NPT II*, a gene in the plasmid vector, was used as an internal control to normalize the transgene insertion site, as described by Kihara et al. (2006).

5.7 | Rhizosphere pH acidification assay

The rhizosphere acidification assay was performed as described by Spartz et al. (2014). Briefly, 10-day pre-grown seedlings were

transferred to -Al (0 μM AlCl₃ at pH 5.0) or Al-rhizotoxic (10 μM AlCl₃ at pH 5.0) solutions for 24 h. After 24 h of stress, the seedlings were transferred to water-agar plates containing .003% bromocresol purple and 30 μM Tris at pH 6.0. Color shifts were observed 12 to 48 h after transfer. These experiments were independently carried out three times, each with three replicates.

5.8 | Organic acid excretion assays

The excretion of malate from the roots was studied as previously described by Kobayashi et al. (2007). The roots of 5 days in vitro pre-grown seedlings were immersed in a modified 2% MGRL medium with or without 10 μM AlCl₃ at pH 5.0 in the presence of 1% sucrose. Vanadate's effect was examined in an Al-containing medium with different concentrations of sodium orthovanadate (Sigma-Aldrich). Root exudates were collected after 24 h, then malate was quantified with the NAD⁺/NADH cycling assay of Hampp et al. (1984) after converting malate to NADH by malate dehydrogenase according to Kobayashi et al. (2007).

5.9 | Morin staining

Morin staining was performed using morin (Sigma-Aldrich, St Louis, USA), as described by Tice et al. (1992). Briefly, Col-0, *almt1*, and *saur55* seedlings were grown for 7 days hydroponically as described above. After 7 days, the seedlings were transferred to an Al-toxic solution (4 μM AlCl₃ at pH 5.0; Ikka et al., 2008) for 24 h. After 24 h of incubation, the roots were stained with morin, as described by Kobayashi et al. (2013). The fluorescence in the root's apex was observed with a fluorescence microscope (Axio Imager.A1; Carl Zeiss, Jena, Germany).

5.10 | Construction of Arabidopsis transgenic lines

SAUR55 promoter::*GUS* transgenic plants were constructed as described by Kobayashi et al. (2014). Briefly, Promoter regions of *SAUR55* from +0 to -2000 (first ATG as 0) were fused with the *β-gluconidase* (*GUS*) and *nopaline synthase* (*NOS*) terminator by overlap-extension PCR (Horton et al., 1989) with specific primers (Table S1). The sequences were cloned into the pBE2113 binary vector (Kobayashi et al., 2014). Simultaneously, *SAUR55*-overexpression and complementation lines were constructed as described by Ohya et al. (2013). *SAUR55* genomic DNA containing the promoter (-2000 from the first ATG) and downstream (+500 from the stop codon) regions were amplified using specific primers (Table S1). The amplified sequence was cloned into the pBE2113 binary vector, which lacks the CaMV35S promoter and *NOS* terminator. PrimeSTAR Max DNA polymerase (Takara Bio, Otsu, Japan) was used for all the PCR steps during vector construction. Positive clones were verified by DNA sequencing using the BigDye Terminator v3.1 Cycle Sequencing kit and ABI

PRISM 3100 Genetic Analyzer (Applied Biosystems, Tokyo, Japan) according to the manufacturer's recommended protocols. The constructs were introduced into *Agrobacterium tumefaciens* strain GV3101 and transformed into Col-0 and STOP1-KO plants by the floral dip method (Clough & Bent, 1998).

5.11 | GUS assays

GUS staining of transgenic lines containing SAUR55 promoter::GUS was performed as described by Kobayashi et al. (2007). Seedlings were grown hydroponically for 10 days followed by treatment with Al (10 μ M AlCl₃ at pH 5.0) for different time periods (3 h, 6 h, and 24 h). After treatments, seedlings were stained for 1 h at 37 °C with a solution containing 1.0 mM X-glucuronide, .1 M Na₃PO₄ buffer (pH 7.0), 10 mM EDTA (pH 8.0), .5 mM K₄Fe(CN)₆ (pH 7.0), .5 mM K₃Fe(CN)₆ (pH 7.0), and .3% Triton X-100. The seedlings were washed, and GUS activity was observed.

5.12 | The localization of SURA55 in onion epidermal cells and BiFC assay in *Nicotiana benthamiana*

The synthetic GFP (sGFP) was fused with the C-terminus of SAUR55 by overlap-extension PCR using the gene-specific primers (Table S1). The PCR fragments were cloned into the pBE2113 vector. 35S::AtPIP2A::mCherry was used as described in Nelson et al. (2007). The DNA transfection and fluorescence observations were performed as described in Fujita et al. (2004). Briefly, The DNA constructs were introduced into onion (*A. cepa* L.) epidermal cells using a pneumatic particle gun. After incubation at 22 °C for 24 h, GFP fluorescence was observed under a fluorescence microscope. The PCR product of SAUR55 and PP2C.D genes amplified by using the gene-specific primers (Table S1) were inserted into multi-cloning site of pSPYNE-35S and pSPYCE-35S (Walter et al., 2004), respectively, to produce pSPYNE-35S-SAUR55 and pSPYCE-35S-PP2C.D2,5,6,7. The constructs were delivered into *A. tumefaciens* strain GV3101 (pMP90) and infiltrated into *Nicotiana benthamiana* as described previously (Sato et al., 2014). Fluorescence was observed in whole mounts using a confocal laser scanning microscope (FV1000, Olympus).

5.13 | Statistical analyses

Statistical analyses were conducted using Microsoft Excel (Microsoft Japan, Tokyo, Japan). All data are expressed as the mean (\pm standard error) of three biological replicates, and three technical replicates were run for each biological replicate. Differences between the parameters were evaluated using the Student's *t*-test, least squared difference test, or Tukey's test. *P*-values < .05 were considered statistically significant.

AUTHOR CONTRIBUTIONS

R.K.A., Y.K., and H.K. conceived and designed the research. R.K.A., Y.K., T.E., T.M., M.S., M.F., and S.I. performed the experiments. R.K.A. and Y.K. analyzed the data. H.K. and Y.K. supervised the study. H.K., Y.K., Y.Y.Y., T.O., Y.F., and M.K. contributed to new reagents or analytical tools. R.K.A., Y.K., and H.K. wrote the manuscript. All authors have approved the manuscript.

ACKNOWLEDGMENTS

The authors are thankful to RIKEN BRC, ABRC, and NASC for providing Arabidopsis seeds. We also thank Riko Hasegawa of Gifu University for growing Arabidopsis during the first stage of this study. We thank Fumie Mori of the RIKEN BRC for establishing the Arabidopsis transgenic line. This work was supported by JSPS KAKENHI Grant Numbers 21H02088 and 19K05753.

CONFLICT OF INTEREST STATEMENT

The authors declare that there are no conflicts of interest.

DATA AVAILABILITY STATEMENT

The data that support the findings of this study are available from the corresponding author upon reasonable request.

ORCID

Takuo Enomoto  <https://orcid.org/0000-0003-2981-7041>

Tasuku Miyachi  <https://orcid.org/0009-0002-8841-5739>

Marie Sakuma  <https://orcid.org/0009-0008-1634-8075>

Miki Fujita  <https://orcid.org/0000-0003-4201-4876>

Takuya Ogata  <https://orcid.org/0000-0003-3361-6234>

Masatomo Kobayashi  <https://orcid.org/0000-0001-9609-4272>

Hiroyuki Koyama  <https://orcid.org/0000-0001-7139-9782>

REFERENCES

- Agrahari, R. K., Enomoto, T., Ito, H., Nakano, Y., Yanase, E., Watanabe, T., Sadhukhan, A., Iuchi, S., Kobayashi, M., Panda, S. K., Yamamoto, Y. Y., Koyama, H., & Kobayashi, Y. (2021). Expression GWAS of *PGIP1* identifies STOP1-dependent and STOP1-independent regulation of *PGIP1* in aluminum stress signaling in Arabidopsis. *Frontiers in Plant Science*, 12, 774687. <https://doi.org/10.3389/fpls.2021.774687>
- Balzergue, C., Dartevelle, T., Godon, C., Laugier, E., Meisrimler, C., Teulon, J. M., Creff, A., Bissler, M., Brouchoud, C., Hagège, A., Müller, J., Chiarenza, S., Javot, H., Becuwe-Linka, N., David, P., Péret, B., Delannoy, E., Thibaud, M. C., Armengaud, J., ... Desnos, T. (2017). Low phosphate activates STOP1-ALMT1 to rapidly inhibit root cell elongation. *Nature Communications*, 8(1), 15300. <https://doi.org/10.1038/ncomms15300>
- Bustin, S. A., Benes, V., Garson, J. A., Hellemans, J., Huggett, J., Kubista, M., Mueller, R., Nolan, T., Pfaffl, M. W., Shipley, G. L., Vandesompele, J., & Wittwer, C. T. (2009). The MIQE guidelines: Minimum information for publication of quantitative real-time PCR experiments. *Clinical Chemistry*, 55(4), 611–622. <https://doi.org/10.1373/clinchem.2008.112797>
- Chan, C., Panzeri, D., Okuma, E., Töldsepp, K., Wang, Y. Y., Louh, G. Y., Chin, T. C., Yeh, Y. H., Yeh, H. L., Yekondi, S., Huang, Y. H., Huang, T. Y., Chiou, T. J., Murata, Y., Kollist, H., & Zimmerli, L. (2020). STRESS INDUCED FACTOR 2 regulates Arabidopsis stomatal immunity through phosphorylation of the Anion Channel SLAC1.



- The Plant Cell*, 32(7), 2216–2236. <https://doi.org/10.1105/tpc.19.00578>
- Clough, S. J., & Bent, A. F. (1998). Floral dip: A simplified method for agrobacterium-mediated transformation of *Arabidopsis thaliana*. *The Plant Journal*, 16(6), 735–743. <https://doi.org/10.1046/j.1365-313x.1998.00343.x>
- Daspute, A. A., Kobayashi, Y., Panda, S. K., Fakrudin, B., Kobayashi, Y., Tokizawa, M., Iuchi, S., Choudhary, A. K., Yamamoto, Y. Y., & Koyama, H. (2018). Characterization of CcSTOP1; a C2H2-type transcription factor regulates Al tolerance gene in pigeonpea. *Planta*, 247(1), 201–214. <https://doi.org/10.1007/s00425-017-2777-6>
- Daspute, A. A., Sadhukhan, A., Tokizawa, M., Kobayashi, Y., Panda, S. K., & Koyama, H. (2017). Transcriptional regulation of aluminum-tolerance genes in higher plants: Clarifying the underlying molecular mechanisms. *Frontiers in Plant Science*, 8, 1358. <https://doi.org/10.3389/fpls.2017.01358>
- Dong, J., Sun, N., Yang, J., Deng, Z., Lan, J., Qin, G., He, H., Deng, X. W., Irish, V. F., Chen, H., & Wei, N. (2019). The transcription factors TCP4 and PIF3 antagonistically regulate organ-specific light induction of SAUR genes to modulate cotyledon opening during de-etiolation in *Arabidopsis*. *The Plant Cell*, 31(5), 1155–1170. <https://doi.org/10.1105/tpc.18.00803>
- Enomoto, T., Tokizawa, M., Ito, H., Iuchi, S., Kobayashi, M., Yamamoto, Y. Y., Kobayashi, Y., & Koyama, H. (2019). STOP1 regulates the expression of HsfA2 and GDHs that are critical for low-oxygen tolerance in *Arabidopsis*. *Journal of Experimental Botany*, 70(12), 3297–3311. <https://doi.org/10.1093/jxb/erz124>
- Eticha, D., Staß, A., & Horst, W. J. (2005). Localization of aluminium in the maize root apex: Can morin detect cell wall-bound aluminium? *Journal of Experimental Botany*, 56(415), 1351–1357. <https://doi.org/10.1093/jxb/eri136>
- Falhof, J., Pedersen, J., Fuglsang, A., & Palmgren, M. (2016). Plasma membrane H⁺-ATPase regulation in the Center of Plant Physiology. *Molecular Plant*, 9(3), 323–337. <https://doi.org/10.1016/j.molp.2015.11.002>
- Fujita, M., Fujita, Y., Maruyama, K., Seki, M., Hiratsu, K., Ohme-Takagi, M., Tran, L., Yamaguchi-Shinozaki, K., & Shinozaki, K. (2004). A dehydration-induced NAC protein, RD26, is involved in a novel ABA-dependent stress-signaling pathway. *The Plant Journal*, 39(6), 863–876. <https://doi.org/10.1111/j.1365-313X.2004.02171.x>
- Hampp, R., Goller, M., & Füllgraf, H. (1984). Determination of compartmented metabolite pools by a combination of rapid fractionation of oat mesophyll protoplasts and Enzymic cycling 1. *Plant Physiology*, 75(4), 1017–1021. <https://doi.org/10.1104/pp.75.4.1017>
- Harper, I. F., Manney, L., DeWitt, N. D., Yoo, M. H., & Sussman, M. R. (1990). The *Arabidopsis thaliana* plasma membrane H⁺-ATPase multigene family. *Journal of Biological Chemistry*, 265, 13601–13608. [https://doi.org/10.1016/S0021-9258\(18\)77391-2](https://doi.org/10.1016/S0021-9258(18)77391-2)
- Haruta, M., Burch, H. L., Nelson, R. B., Barrett-Wilt, G., Kline, K. G., Mohsin, S. B., Young, J. C., Otegui, M. S., & Sussman, M. R. (2010). Molecular characterization of mutant *Arabidopsis* plants with reduced plasma membrane proton pump activity. *Journal of Biological Chemistry*, 285, 17918–17929. <https://doi.org/10.1074/jbc.M110.101733>
- Hoekenga, O., Maron, L., Piñeros, M., Cañado, G., Shaff, J., Kobayashi, Y., Ryan, P., Dong, B., Delhaize, E., Sasaki, T., Matsumoto, H., Yamamoto, Y., Koyama, H., & Kochian, L. V. (2006). AtALMT1, which encodes a malate transporter, is identified as one of several genes critical for aluminum tolerance in *Arabidopsis*. *Proceedings of the National Academy of Sciences*, 103(25), 9738–9743. <https://doi.org/10.1073/pnas.0602868103>
- Hong, J. K., Choi, D. S., Kim, S. H., Yi, S. Y., Kim, Y. J., & Hwang, B. K. (2008). Distinct roles of the pepper pathogen-induced membrane protein gene CaPIMP1 in bacterial disease resistance and oomycete disease susceptibility. *Planta*, 228, 485–497. <https://doi.org/10.1007/s00425-008-0752-y>
- Horton, R. M., Hunt, H. D., Ho, S. N., Pullen, J. K., & Pease, L. R. (1989). Engineering hybrid genes without the use of restriction enzymes: Gene splicing by overlap extension. *Gene*, 77(1), 61–68. [https://doi.org/10.1016/0378-1119\(89\)90359-4](https://doi.org/10.1016/0378-1119(89)90359-4)
- Huang, C. F., Yamaji, N., Mitani, N., Yano, M., Nagamura, Y., & Ma, J. F. (2009). A bacterial-type ABC transporter is involved in aluminum tolerance in rice. *The Plant Cell*, 21(2), 655–667. <https://doi.org/10.1105/tpc.108.064543>
- Ikka, T., Kobayashi, Y., Tazib, T., & Koyama, H. (2008). Aluminum-tolerance QTL in Columbia/Kashmir inbred population of *Arabidopsis thaliana* is not associated with aluminum-responsive malate excretion. *Plant Science*, 175(4), 533–538. <https://doi.org/10.1016/j.plantsci.2008.06.001>
- Ito, H., Kobayashi, Y., Yamamoto, Y., & Koyama, H. (2019). Characterization of NtSTOP1-regulating genes in tobacco under aluminum stress. *Soil Science and Plant Nutrition*, 65(3), 251–258. <https://doi.org/10.1080/00380768.2019.1603064>
- Iuchi, S., Koyama, H., Iuchi, A., Kobayashi, Y., Kitabayashi, S., Kobayashi, Y., Ikka, T., Hirayama, T., Shinozaki, K., & Kobayashi, M. (2007). Zinc finger protein STOP1 is critical for proton tolerance in *Arabidopsis* and coregulates a key gene in aluminum tolerance. *Proceedings of the National Academy of Sciences*, 104(23), 9900–9905. <https://doi.org/10.1073/pnas.0700117104>
- Kihara, T., Zhao, C. R., Kobayashi, Y., Takita, E., Kawazu, T., & Koyama, H. (2006). Simple identification of transgenic *Arabidopsis* plants carrying a single copy of the integrated gene. *Bioscience, Biotechnology, and Biochemistry*, 70(7), 1780–1783. <https://doi.org/10.1271/bbb.50687>
- Kobayashi, Y., Hoekenga, O. A., Itoh, H., Nakashima, M., Saito, S., Shaff, J. E., Maron, L. G., Piñeros, M. A., Kochian, L. V., & Koyama, H. (2007). Characterization of AtALMT1 expression in aluminum-inducible malate release and its role for rhizotoxic stress tolerance in *Arabidopsis*. *Plant Physiology*, 145(3), 843–852. <https://doi.org/10.1104/pp.107.102335>
- Kobayashi, Y., Kobayashi, Y., Sugimoto, M., Lakshmanan, V., Iuchi, S., Kobayashi, M., Bais, H. P., & Koyama, H. (2013). Characterization of the complex regulation of AtALMT1 expression in response to phytohormones and other inducers. *Plant Physiology*, 162(2), 732–740. <https://doi.org/10.1104/pp.113.218065>
- Kobayashi, Y., Kobayashi, Y., Watanabe, T., Shaff, J. E., Ohta, H., Kochian, L. V., Wagatsuma, T., Kinraide, T. B., & Koyama, H. (2013). Molecular and physiological analysis of Al³⁺ and H⁺ rhizotoxicities at moderately acidic conditions. *Plant Physiology*, 163(1), 180–192. <https://doi.org/10.1104/pp.113.222893>
- Kobayashi, Y., Ohyama, Y., Kobayashi, Y., Ito, H., Iuchi, S., Fujita, M., Zhao, C.-R., Tanveer, T., Ganesan, M., Kobayashi, M., & Koyama, H. (2014). STOP2 activates transcription of several genes for Al- and low pH-tolerance that are regulated by STOP1 in *Arabidopsis*. *Molecular Plant*, 7(2), 311–322. <https://doi.org/10.1093/mp/sst116>
- Kochian, L. V., Piñeros, M., Liu, J., & Magalhaes, J. (2015). Plant adaptation to acid soils: The molecular basis for crop aluminum resistance. *Annual Review of Plant Biology*, 66(1), 571–598. <https://doi.org/10.1146/annurev-arplant-043014-114822>
- Kusunoki, K., Nakano, Y., Tanaka, K., Sakata, Y., Koyama, H., & Kobayashi, Y. (2017). Transcriptomic variation among six *Arabidopsis thaliana* accessions identified several novel genes controlling aluminum tolerance. *Plant, Cell & Environment*, 40(2), 249–263. <https://doi.org/10.1111/pce.12866>
- Kyte, J., & Doolittle, R. F. (1982). A simple method for displaying the hydropathic character of a protein. *Journal of Molecular Biology*, 157(1), 105–132. [https://doi.org/10.1016/0022-2836\(82\)90515-0](https://doi.org/10.1016/0022-2836(82)90515-0)
- Larsen, P. B., Geisler, M. J., Jones, C. A., Williams, K. M., & Cancel, J. D. (2005). ALS3 encodes a phloem-localized ABC transporter-like

- protein that is required for aluminum tolerance in Arabidopsis. *The Plant Journal*, 41(3), 353–363. <https://doi.org/10.1111/j.1365-313X.2004.02306.x>
- Liu, J., Magalhaes, J., Shaff, J., & Kochian, L. V. (2009). Aluminum-activated citrate and malate transporters from the MATE and ALMT families function independently to confer Arabidopsis aluminum tolerance. *The Plant Journal*, 57(3), 389–399. <https://doi.org/10.1111/j.1365-313X.2008.03696>
- Liu, J., Piñeros, M., & Kochian, L. V. (2014). The role of aluminum sensing and signaling in plant aluminum resistance. *Journal of Integrative Plant Biology*, 56(3), 221–230. <https://doi.org/10.1111/jipb.12162>
- Mercier, C., Roux, B., Have, M., Le Poder, L., Duong, N., David, P., Leonhardt, N., Blanchard, L., Naumann, C., Abel, S., Cuyas, L., Pluchon, S., Nussaume, L., & Desnos, T. (2021). Root responses to aluminium and iron stresses require the SIZ1 SUMO ligase to modulate the STOP1 transcription factor. *The Plant Journal*, 108(5), 1507–1521. <https://doi.org/10.1111/tj.15525>
- Młodzinska-Michta, E. (2022). Root system responses to phosphate nutrition involve plasma membrane H⁺-ATPases in Arabidopsis thaliana. *Acta Physiologiae Plantarum*, 44, 76. <https://doi.org/10.1007/s11738-022-03413-7>
- Murashige, T., & Skoog, F. (1962). A revised medium for rapid growth and bioassays with tobacco tissue cultures. *Physiologia Plantarum*, 15(3), 473–497. <https://doi.org/10.1111/j.1399-3054.1962.tb08052.x>
- Nakano, Y., Kusunoki, K., Hoekenga, O., Tanaka, K., Iuchi, S., Sakata, Y., Kobayashi, M., Yamamoto, Y., Koyama, H., & Kobayashi, Y. (2020). Genome-wide association study and genomic prediction elucidate the distinct genetic architecture of aluminum and proton tolerance in Arabidopsis thaliana. *Frontiers in Plant Science*, 11, 405. <https://doi.org/10.3389/fpls.2020.00405>
- Nakano, Y., Kusunoki, K., Maruyama, H., Enomoto, T., Tokizawa, M., Iuchi, S., Kobayashi, M., Kochian, L., Koyama, H., & Kobayashi, Y. (2020). A single-population GWAS identified AtMATE expression level polymorphism caused by promoter variants is associated with variation in aluminum tolerance in a local Arabidopsis population. *Plant Direct*, 4(8), e250. <https://doi.org/10.1002/pld3.250>
- Nelson, B., Cai, X., & Nebenführ, A. (2007). A multicolored set of in vivo organelle markers for co-localization studies in Arabidopsis and other plants. *The Plant Journal*, 51(6), 1126–1136. <https://doi.org/10.1111/j.1365-313X.2007.03212.x>
- Neumann, G., Massonneau, A., Martinoia, E., & Römheld, V. (1999). Physiological adaptations to phosphorus deficiency during proteoid root development in white lupin. *Planta*, 208(3), 373–382. <https://doi.org/10.1007/s004250050572>
- Obayashi, T., Hibara, H., Kagaya, Y., Aoki, Y., & Kinoshita, K. (2022). ATTED-II v11: A plant gene coexpression database using a sample balancing technique by subagging of principal components. *Plant & Cell Physiology*, 63(6), 869–881. <https://doi.org/10.1093/pcp/pcac041>
- Ohno, T., Koyama, H., & Hara, T. (2003). Characterization of citrate transport through the plasma membrane in a carrot mutant cell line with enhanced citrate excretion. *Plant and Cell Physiology*, 44(2), 156–162. <https://doi.org/10.1093/pcp/pcg025>
- Ohno, T., Nakahira, S., Suzuki, Y., Kani, T., Hara, T., & Koyama, H. (2004). Molecular characterization of plasma membrane H⁺-ATPase in a carrot mutant cell line with enhanced citrate excretion. *Physiologia Plantarum*, 122(2), 265–274. <https://doi.org/10.1111/j.1399-3054.2004.00399.x>
- Ohyama, Y., Ito, H., Kobayashi, Y., Ikka, T., Morita, A., Kobayashi, M., Imaizumi, R., Aoki, T., Komatsu, K., Sakata, Y., Iuchi, S., & Koyama, H. (2013). Characterization of AtSTOP1 orthologous genes in tobacco and other plant species. *Plant Physiology*, 162(4), 1937–1946. <https://doi.org/10.1104/pp.113.218958>
- O'Malley, R. C., Huang, S., Song, L., Lewsey, M. G., Bartlett, A., Nery, J. R., Galli, M., Gallavotti, A., & Ecker, J. R. (2016). Cistrome and epistrome features shape the regulatory DNA landscape. *Cell*, 165(5), 1280–1292. <https://doi.org/10.1016/j.cell.2016.04.038>
- Palmgren, M. G. (2001). Plant plasma membrane H⁺-ATPases: Powerhouses for nutrient uptake. *Annual Review of Plant Physiology and Plant Molecular Biology*, 52(1), 817–845. <https://doi.org/10.1146/annurev.arplant.52.1.817>
- Qiu, T., Qi, M., Ding, X., Zheng, Y., Zhou, T., Chen, Y., Han, N., Zhu, M., Bian, H., & Wang, J. (2020). The SAUR41 subfamily of SMALL AUXIN UP RNA genes is abscisic acid inducible to modulate cell expansion and salt tolerance in Arabidopsis thaliana seedlings. *Annals of Botany*, 125(5), 805–819. <https://doi.org/10.1093/aob/mcz160>
- Ren, H., & Gray, W. M. (2015). SAUR proteins as effectors of hormonal and environmental signals in plant growth. *Molecular Plant*, 8(8), 1153–1164. <https://doi.org/10.1016/j.molp.2015.05.003>
- Ren, H., Park, M., Spartz, A., Wong, J., & Gray, W. M. (2018). A subset of plasma membrane-localized PP2C.D phosphatases negatively regulate SAUR-mediated cell expansion in Arabidopsis. *PLoS Genetics*, 14(6), e1007455. <https://doi.org/10.1371/journal.pgen.1007455>
- Rico-Reséndiz, F., Cervantes-Pérez, S. A., Espinal-Centeno, A., Dipp-Álvarez, M., Oropeza-Aburto, A., Hurtado-Bautista, E., Cruz-Hernández, A., Bowman, J. L., Ishizaki, K., Arteaga-Vázquez, M. A., Herrera-Estrella, L., & Cruz-Ramírez, A. (2020). Transcriptional and morpho-physiological responses of Marchantia polymorpha upon phosphate starvation. *International Journal of Molecular Sciences*, 21(21), 8354. <https://doi.org/10.3390/ijms21218354>
- Sadhukhan, A., Agrahari, R. K., Wu, L., Watanabe, T., Nakano, Y., Panda, S. K., Koyama, H., & Kobayashi, Y. (2021). Expression genome-wide association study identifies that phosphatidylinositol-derived signalling regulates ALUMINIUM SENSITIVE3 expression under aluminium stress in the shoots of Arabidopsis thaliana. *Plant Science*, 302, 110711. <https://doi.org/10.1016/j.plantsci.2020.110711>
- Sadhukhan, A., Kobayashi, Y., Iuchi, S., & Koyama, H. (2021). Synergistic and antagonistic pleiotropy of STOP1 in stress tolerance. *Trends in Plant Science*, 26(10), 1014–1022. <https://doi.org/10.1016/j.tplants.2021.06.011>
- Sato, H., Mizoi, J., Tanaka, H., Maruyama, K., Qin, F., Osakabe, Y., Morimoto, K., Otori, T., Kusakabe, K., Nagata, M., & Shinozaki, K. (2014). Arabidopsis DPB3-1, a DREB2A interactor, specifically enhances heat stress-induced gene expression by forming a heat stress-specific transcriptional complex with NF-Y subunits. *The Plant Cell*, 26(12), 4954–4973. <https://doi.org/10.1105/tpc.114.132928>
- Sawaki, Y., Iuchi, S., Kobayashi, Y., Kobayashi, Y., Ikka, T., Sakurai, N., Fujita, M., Shinozaki, K., Shibata, D., Kobayashi, M., & Koyama, H. (2009). STOP1 regulates multiple genes that protect Arabidopsis from proton and aluminum toxicities. *Plant Physiology*, 150(1), 281–294. <https://doi.org/10.1104/pp.108.134700>
- Sawaki, Y., Kobayashi, Y., Kihara-Doi, T., Nishikubo, N., Kawazu, T., Kobayashi, M., Kobayashi, Y., Iuchi, S., Koyama, H., & Sato, S. (2014). Identification of a STOP1-like protein in eucalyptus that regulates transcription of Al tolerance genes. *Plant Science*, 223, 8–15. <https://doi.org/10.1016/j.plantsci.2014.02.011>
- Shen, H., He, L. F., Sasaki, T., Yamamoto, Y., Zheng, S. J., Ligaba, A., Yan, X. L., Ahn, S. J., Yamaguchi, M., Sasakawa, H., & Matsumoto, H. (2005). Citrate secretion coupled with the modulation of soybean root tip under aluminum stress. Up-regulation of transcription, translation, and threonine-oriented phosphorylation of plasma membrane H⁺-ATPase. *Plant Physiology*, 138(1), 287–296. <https://doi.org/10.1104/pp.104.058065>
- Siao, W., Coskun, D., Baluška, F., Kronzucker, H. J., & Xu, W. (2020). Root-apex proton fluxes at the Centre of soil-stress acclimation. *Trends in*



- Plant Science*, 25(8), 794–804. <https://doi.org/10.1016/j.tplants.2020.03.002>
- Spartz, A. K., Lee, S. H., Wenger, J. P., Gonzalez, N., Itoh, H., Inzé, D., Peer, W. A., Murphy, A. S., Overvoorde, P. J., & Gray, W. M. (2012). The SAUR19 subfamily of SMALL AUXIN UP RNA genes promote cell expansion. *The Plant Journal*, 70(6), 978–990. <https://doi.org/10.1111/j.1365-313X.2012.04946.x>
- Spartz, A. K., Ren, H., Park, M. Y., Grandt, K. N., Lee, S. H., Murphy, A. S., Sussman, M. R., Overvoorde, P. J., & Gray, W. M. (2014). SAUR inhibition of PP2C-D phosphatases activates plasma membrane H⁺-ATPases to promote cell expansion in Arabidopsis. *The Plant Cell*, 26(5), 2129–2142. <https://doi.org/10.1105/tpc.114.126037>
- Stortenbeker, N., & Bemer, M. (2019). The SAUR gene family: The plant's toolbox for adaptation of growth and development. *Journal of Experimental Botany*, 70(1), 17–27. <https://doi.org/10.1093/jxb/ery332>
- Tamura, K., Stecher, G., Peterson, D., Filipowski, A., & Kumar, S. (2013). MEGA6: Molecular evolutionary genetics analysis version 6.0. *Molecular Biology and Evolution*, 30(12), 2725–2729. <https://doi.org/10.1093/molbev/mst197>
- Tice, K. R., Parker, D. R., & DeMason, D. A. (1992). Operationally defined apoplastic and symplastic aluminum fractions in root tips of aluminum-intoxicated wheat. *Plant Physiology*, 100(1), 309–318. <https://doi.org/10.1104/pp.100.1.309>
- Toda, T., Koyama, H., & Hara, T. (1999). A simple hydroponic culture method for the development of a highly viable root system in Arabidopsis thaliana. *Bioscience, Biotechnology, and Biochemistry*, 63(1), 210–212. <https://doi.org/10.1271/bbb.63.210>
- Tokizawa, M., Enomoto, T., Ito, H., Wu, L., Kobayashi, Y., Mora-Macías, J., Armenta-Medina, D., Iuchi, S., Kobayashi, M., Nomoto, M., Tada, Y., Fujita, M., Shinozaki, K., Yamamoto, Y. Y., Kochian, L. V., & Koyama, H. (2021). High affinity promoter binding of STOP1 is essential for early expression of novel aluminum-induced resistance genes GDH1 and GDH2 in Arabidopsis. *Journal of Experimental Botany*, 72(7), 2769–2789. <https://doi.org/10.1093/jxb/erab031>
- Tokizawa, M., Kobayashi, Y., Saito, T., Kobayashi, M., Iuchi, S., Nomoto, M., Tada, Y., Yamamoto, Y. Y., & Koyama, H. (2015). Sensitive to proton rhizotoxicity1, calmodulin binding transcription activator2, and other transcription factors are involved in aluminum-activated malate transporter1 expression. *Plant Physiology*, 167(3), 991–1003. <https://doi.org/10.1104/pp.114.256552>
- Tomasi, N., Kretzschmar, T., Espen, L., Weisskopf, L., Fuglsang, A. T., Palmgren, M. G., Neumann, G., Varanini, Z., Pinton, R., Martinoia, E., & Cesco, S. (2009). Plasma membrane H⁺-ATPase-dependent citrate exudation from cluster roots of phosphate-deficient white lupin. *Plant, Cell & Environment*, 32(5), 465–475. <https://doi.org/10.1111/j.1365-3040.2009.01938.x>
- Tsutsui, T., Yamaji, N., & Ma, F. (2011). Identification of a cis-acting element of ART1, a C2H2-type zinc-finger transcription factor for aluminum tolerance in rice. *Plant Physiology*, 156(2), 925–931. <https://doi.org/10.1104/pp.111.175802>
- Walker, D. J., Black, C. R., & Miller, A. J. (1998). The role of cytosolic potassium and pH in the growth of barley roots. *Plant Physiology*, 118(3), 957–964. <https://doi.org/10.1104/pp.118.3.957>
- Walter, M., Chaban, C., Schütze, K., Batistic, O., Weckermann, K., Näke, C., Blazevic, D., Grefen, C., Schumacher, K., Oecking, C., & Harter, K. (2004). Visualization of protein interactions in living plant cells using bimolecular fluorescence complementation. *The Plant Journal*, 40(3), 428–438. <https://doi.org/10.1111/j.1365-313X.2004.02219.x>
- Wang, Z., Yang, L., Liu, Z., Lu, M., Wang, M., Sun, Q., Lan, Y., Shi, T., Wu, D., & Hua, J. (2019). Natural variations of growth thermo-responsiveness determined by SAUR 26/27/28 proteins in Arabidopsis thaliana. *New Phytologist*, 224(1), 291–305. <https://doi.org/10.1111/nph.15956>
- Wang, Z., Yang, L., Wu, D., Zhang, N., & Hua, J. (2021). Polymorphisms in cis-elements confer SAUR26 gene expression difference for thermo-response natural variation in Arabidopsis. *New Phytologist*, 229(5), 2751–2764. <https://doi.org/10.1111/nph.17078>
- Wong, J. H., Klejchová, M., Snipes, S. A., Nagpal, P., Bak, G., Wang, B., Dunlap, S., Park, M. Y., Kunkel, E. N., Trinidad, B., Reed, J. W., Blatt, M. R., & Gray, W. M. (2021). SAUR proteins and PP2C.D phosphatases regulate H⁺-ATPases and K⁺ channels to control stomatal movements. *Plant Physiology*, 185(1), 256–273. <https://doi.org/10.1093/plphys/kiaa023>
- Wu, L., Kobayashi, Y., Wasaki, J., & Koyama, H. (2018). Organic acid excretion from roots: A plant mechanism for enhancing phosphorus acquisition, enhancing aluminum tolerance, and recruiting beneficial rhizobacteria. *Soil Science and Plant Nutrition*, 64(6), 697–704. <https://doi.org/10.1080/00380768.2018.1537093>
- Wu, L., Sadhukhan, A., Kobayashi, Y., Ogo, N., Tokizawa, M., Agrahari, R. K., Ito, H., Iuchi, S., Kobayashi, M., Asai, A., & Koyama, H. (2019). Involvement of phosphatidylinositol metabolism in aluminum-induced malate secretion in Arabidopsis. *Journal of Experimental Botany*, 70(12), 3329–3342. <https://doi.org/10.1093/jxb/erz179>
- Xie, W., Liu, S., Gao, H., Wu, J., Liu, D., Kinoshita, T., & Huang, C. F. (2023). PP2C. D phosphatase SAL1 positively regulates aluminum resistance via restriction of aluminum uptake in rice. *Plant Physiology*, 192(2), 1498–1516. <https://doi.org/10.1093/plphys/kiad122>
- Xu, J., Zhu, J., Liu, J., Wang, J., Ding, Z., & Tian, H. (2021). SIZ1 negatively regulates aluminum resistance by mediating the STOP1-ALMT1 pathway in Arabidopsis. *Journal of Integrative Plant Biology*, 63(6), 1147–1160. <https://doi.org/10.1111/jipb.13091>
- Yamaji, N., Huang, C. F., Nagao, S., Yano, M., Sato, Y., Nagamura, Y., & Ma, J. F. (2009). A zinc finger transcription factor ART1 regulates multiple genes implicated in aluminum tolerance in rice. *The Plant Cell*, 21(10), 3339–3349. <https://doi.org/10.1105/tpc.109.070771>
- Yan, F., Zhu, Y., Muller, C., Zörb, C., & Schubert, S. (2002). Adaptation of H⁺-pumping and plasma membrane H⁺ ATPase activity in proteoid roots of white lupin under phosphate deficiency. *Plant Physiology*, 129(1), 50–63. <https://doi.org/10.1104/pp.010869>
- Yang, T., & Poovaiah, B. W. (2002). A calmodulin-binding/CGCG box DNA-binding protein family involved in multiple signaling pathways in plants. *Journal of Biological Chemistry*, 277(47), 45049–45058. <https://doi.org/10.1074/jbc.m207941200>
- Yu, W., Kan, Q., Zhang, J., Zeng, B., & Chen, Q. (2016). Role of the plasma membrane H⁺-ATPase in the regulation of organic acid exudation under aluminum toxicity and phosphorus deficiency. *Plant Signaling & Behavior*, 11(1), e1106660. <https://doi.org/10.1080/15592324.2015.1106660>
- Yuan, W., Zhang, D., Song, T., Xu, F., Lin, S., Xu, W., Li, Q., Zhu, Y., Liang, J., & Zhang, J. (2017). Arabidopsis plasma membrane H⁺-ATPase genes AHA2 and AHA7 have distinct and overlapping roles in the modulation of root tip H⁺ efflux in response to low-phosphorus stress. *Journal of Experimental Botany*, 68(7), 1731–1741. <https://doi.org/10.1093/jxb/erx040>
- Zhang, J., Wei, J., Li, D., Kong, X., Rengel, Z., Chen, L., Yang, Y., Cui, X., & Chen, Q. (2017). The role of the plasma membrane H⁺-ATPase in plant responses to aluminum toxicity. *Frontiers in Plant Science*, 8, 1757. <https://doi.org/10.3389/fpls.2017.01757>
- Zhang, F., Yan, X., Han, X., Tang, R., Chu, M., Yang, Y., Yang, Y. H., Zhao, F., Fu, A., Luan, S., & Lan, W. (2019). A defective vacuolar proton pump enhances aluminum tolerance by reducing vacuole sequestration of organic acids. *Plant Physiology*, 181(2), 743–761. <https://doi.org/10.1104/pp.19.00626>

- Zhang, H., Yu, Z., Yao, X., Chen, J., Chen, X., Zhou, H., Lou, Y., Ming, F., & Jin, Y. (2021). Genome-wide identification and characterization of small auxin-up RNA (SAUR) gene family in plants: Evolution and expression profiles during normal growth and stress response. *BMC Plant Biology*, 21(1), 4. <https://doi.org/10.1186/s12870-020-02781-x>
- Zhang, Y., Zhang, J., Guo, J., Zhou, F., Singh, S., Xu, X., Xie, Q., Yang, Z., & Huang, C. F. (2019). F-box protein RAE1 regulates the stability of the aluminum-resistance transcription factor STOP1 in Arabidopsis. *Proceedings of the National Academy of Sciences*, 116(1), 319–327. <https://doi.org/10.1073/pnas.1814426116>
- Zhou, H., Guan, W., Zhou, M., Shen, J., Liu, X., Wu, D., Yin, X., & Xie, Y. (2020). Cloning and characterization of a gene encoding true D-cysteine desulfhydrase from *Oryza sativa*. *Plant Molecular Biology Reporter*, 38(1), 95–113. <https://doi.org/10.1007/s11105-019-01181-2>

SUPPORTING INFORMATION

Additional supporting information can be found online in the Supporting Information section at the end of this article.

How to cite this article: Agrahari, R. K., Kobayashi, Y., Enomoto, T., Miyachi, T., Sakuma, M., Fujita, M., Ogata, T., Fujita, Y., Iuchi, S., Kobayashi, M., Yamamoto, Y. Y., & Koyama, H. (2024). STOP1-regulated *SMALL AUXIN UP RNA55* (*SAUR55*) is involved in proton/malate co-secretion for Al tolerance in Arabidopsis. *Plant Direct*, 8(1), e557. <https://doi.org/10.1002/pld3.557>